NATIONAL ENERGY TECHNOLOGY LABORATORY

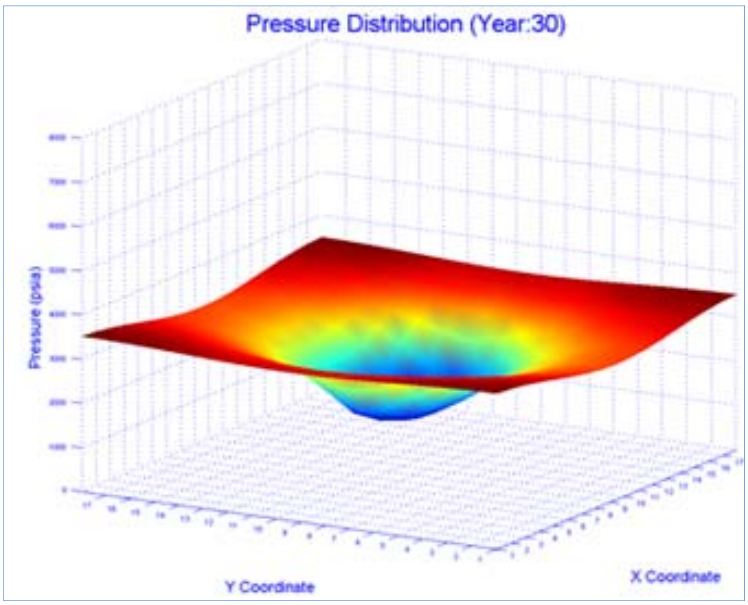

Investigation of CO_2 Storage and Enhanced Gas Recovery in Depleted Shale Gas Formations Using a Dual-Porosity/Dual-Permeability, Multiphase Reservoir Simulator

25 September 2014

U.S. DEPARTMENT OF ENERGY

Office of Fossil Energy

NETL-TRS-4-2014

Disclaimer

This report was prepared as an account of work sponsored by an agency of the United States Government. Neither the United States Government nor any agency thereof, nor any of their employees, makes any warranty, express or implied, or assumes any legal liability or responsibility for the accuracy, completeness, or usefulness of any information, apparatus, product, or process disclosed, or represents that its use would not infringe privately owned rights. Reference therein to any specific commercial product, process, or service by trade name, trademark, manufacturer, or otherwise does not necessarily constitute or imply its endorsement, recommendation, or favoring by the United States Government or any agency thereof. The views and opinions of authors expressed therein do not necessarily state or reflect those of the United States Government or any agency thereof.

Cover Illustration: Simulated pressure distribution after 30 years of natural gas production from a fractured shale formation shows depletion in the stimulated reservoir volume around a multi-stage lateral before CO_2 injection is initiated.

Suggested Citation: Kulga, B.; Dilmore, R.; Wyatt, C.; Ertekin, T. *Investigation of CO_2 Storage and Enhanced Gas Recovery in Depleted Shale Gas Formations Using a Dual-Porosity/Dual-Permeability, Multiphase Reservoir Simulator*; NETL-TRS-4-2014; NETL Technical Report Series; U.S. Department of Energy, National Energy Technology Laboratory: Morgantown, WV, 2014; p 72.

An electronic version of this report can be found at:

http://www.netl.doe.gov/research/on-site-research/publications/featured-technical-reports

Investigation of CO_2 Storage and Enhanced Gas Recovery in Depleted Shale Gas Formations Using a Dual-Porosity/Dual-Permeability, Multiphase Reservoir Simulator

Burak Kulga[1], Robert Dilmore[2], Christopher Wyatt[3], Turgay Ertekin[1]

[1] Penn State University, 201 Old Main, University Park, PA 16802

[2] U.S. Department of Energy, Office of Research and Development, National Energy Technology Laboratory, 626 Cochrans Mill Road, Pittsburgh, PA 15236

[3] U.S. Department of Energy, National Energy Technology Laboratory, Sextant Technical Services, 3610 Collins Ferry Road, Morgantown, WV 26507

NETL-TRS-4-2014

25 September 2014

NETL Contacts:

Robert Dilmore, Technical Coordinator

George Richards, ICMI Technology Director

George Guthrie, Geologic & Environmental Sciences Focus Area Lead

This page intentionally left blank.

Table of Contents

EXECUTIVE SUMMARY 1
1. DEVELOPMENT OF THE PSU-SHALECOMP SIMULATOR 4
1.1 DEVELOPING CAPABILITIES OF THE RESERVOIR SIMULATOR (PSU-SHALECOMP) 4
1.2 COMPUTER RUNS TO STUDY THE PRODUCTION PERFORMANCE OF A REGIONAL TYPICAL SHALE GAS RESERVOIR USING PSU-SHALECOMP SIMULATOR 4
1.3 DESIGNING PRELIMINARY RUNS INVOLVING CO_2 INJECTION 10
1.4 WELL-SPACING/PATTERN OPTIONS STUDIED TO UNDERSTAND THE CO_2 FLOW BEHAVIOR IN NANODARCY SHALE FORMATIONS 16
1.5 SIMULATIONS WITH DIFFERENT WELL PATTERNS WITH POSSIBLE FRACTURE ('FRAC') HITS TO THE NEIGHBORING WELLS 16
2. HISTORY MATCHING OF NORMALIZED FIELD DATA 21
2.1 LOW-RATE CASE INITIAL PRODUCTION 22
2.2 MID-RATE CASE INITIAL PRODUCTION 24
2.3 HIGH-RATE CASE INITIAL PRODUCTION 27
2.4 CONCLUSIONS 29
3. VARYING THE CO_2 INJECTION RATE AND LANGMUIR PRESSURES/VOLUMES 30
3.1 VARYING THE CO_2 INJECTION RATE FOR THE MID-RATE CASE 31
3.2 MODEL INTEGRATION OF WEATHERFORD LANGMUIR PRESSURES AND VOLUMES 31
4. PARAMETRIC STUDY OF FOUR PROJECT DESIGN PARAMETERS 34
4.1 HORIZONTAL WELLBORE LENGTH 34
4.2 SRV FRACTURE PERMEABILITY 35
4.3 SRV FRACTURE POROSITY 35
4.4 SRV FRACTURE SPACING 36
5. THE EFFECT OF ALLOWING PERMEABILITY MODIFICATION AS A FUNCTION OF PORE PRESSURE WITHIN THE PSU-SHALECOMP MODEL 37
6. MONTE CARLO SIMULATION STUDIES AND OTHER SENSITIVITY ANALYSES 40
6.1 INITIAL MONTE CARLO SIMULATION STUDY 40
6.2 DETAILED MONTE CARLO SIMULATIONS 40
6.3 GRID SIZE SENSITIVITY 44
6.4 PRODUCTION/INJECTION PERFORMANCE FOR DIFFERENT HWLS AND WING SIZE 45
6.5 PRODUCTION/INJECTION PERFORMANCE FOR DIFFERENT HYDRAULIC FRACTURE SPACING IN THE SRV ZONE 47
7. HISTORY MATCHING OF FIELD DATA FOR A SINGLE-LATERAL PAD 48
7.1 DAILY AND CUMULATIVE GAS PRODUCTION 48
7.2 CO_2 BREAKTHROUGH TIME 50
8. REFERENCES 52

List of Figures

Figure 1: Cumulative production performance of unstimulated horizontal wells. 5
Figure 2: Cumulative production performance of stimulated horizontal wells (areal extent of SRV: 18 acres). 6
Figure 3: Cumulative production performance of stimulated horizontal wells (areal extent of SRV: 36 acres). 6
Figure 4: Cumulative production performance of different SRVs (HWL = 1,800 ft). 7
Figure 5: Cumulative production performance of different SRVs (HWL = 2,200 ft). 8
Figure 6: Cumulative production performance of different SRVs (HWL = 2,600 ft). 8
Figure 7: Daily gas production for stimulated wells. 9
Figure 8: Daily gas production for unstimulated wells. 10
Figure 9: Scenario definition used in CO_2 injection sensitivity simulations: parameter values and model well pattern configuration. 11
Figure 10: Simulation 1: (a) daily production rate, (b) cumulative production, (c) final pressure distribution, and (d) final CO_2 concentration distribution. 12
Figure 11: Simulation 2: (a) daily production rate, (b) cumulative production, (c) final pressure distribution, and (d) final CO_2 concentration distribution. 13
Figure 12: Simulation 3: (a) daily production rate, (b) cumulative production, (c) final pressure distribution, and (d) final CO_2 concentration distribution. 14
Figure 13: Simulation 4: (a) daily production rate, (b) cumulative production, (c) final pressure distribution, and (d) final CO_2 concentration distribution. 15
Figure 14: Pressure distributions of CMG (left) and PSU-SHALECOMP (right) at year 30. 16
Figure 15: Case 1, CO_2 production investigation at the center well (connectivity between the wells exists). 17
Figure 16: Case 2, CO_2 production investigation at the center well (connectivity between the wells does not exist). 18
Figure 17: Case 3, CO_2 production investigation at the center well (connectivity between the wells exists). 19
Figure 18: Case 4, CO_2 production investigation at the center well (connectivity between the wells does not exist). 20
Figure 19: Data used for low-rate, mid-rate, and high-rate simulations. 22
Figure 20: Low-rate case history match. 23
Figure 21: Low-rate case pressure distribution. 24
Figure 22: Mid-rate case history match. 25
Figure 23: Mid-rate case pressure distribution. 25
Figure 24: Mid-rate case production and injection performance. 26
Figure 25: High-rate case history match. 27
Figure 26: High-rate case production and injection performance. 28
Figure 27: Mole fraction of CO_2 in the matrix and the fracture. 29
Figure 28: Production performances using varied CO_2 injection rates. 30
Figure 29: Cumulative production values and desorption fractions for mid-rate case at 4,500 psi. 32
Figure 30: Effect of varying HWL on production when using the mid-rate case. 34
Figure 31: Effect of varying fracture permeability on production when using the mid-rate case. 35
Figure 32: Effect of varying fracture porosity on production when using the mid-rate case. 36

Figure 33: Effect of varying fracture porosity on production when using the mid-rate case. 36
Figure 34: Effect of net stress on average permeability. 37
Figure 35: Effect of permeability modification on production performance..... 38
Figure 36: Detailed Monte Carlo simulation at constant pressure (5,000 psi) - 1 frequency function: (a) OGIP, (b) cumulative CH_4 production, and (c) cumulative CO_2 injection..... 41
Figure 37: Detailed Monte Carlo simulation at constant pressure (5,000 psi) - 1 frequency function: (a) OGIP, (b) cumulative CH_4 production, and (c) cumulative CO_2 injection..... 42
Figure 38: Detailed Monte Carlo simulation at constant injection rate (1.5 MMSCFD) - 1 frequency function: (a) OGIP, (b) cumulative CH_4 production, and (c) cumulative CO_2 injection..... 43
Figure 39: Detailed Monte Carlo simulation at constant injection rate (1.5 MMSCFD) - 1 distribution function: (a) OGIP, (b) cumulative CH_4 production, and (c) cumulative CO_2 injection..... 44
Figure 40: Illustration of model sensitivity to varying grid block size on a) lateral gas production profile, and b) formation pressure distribution. 45
Figure 41: Single-lateral pad, Simulation 1 production performance..... 48
Figure 42: Single-lateral pad, Simulation 2 production performance..... 48
Figure 43: Single-lateral pad, Simulation 3 production performance..... 49
Figure 44: Single-lateral pad, Simulation 4 production performance..... 49
Figure 45: Top view of Model 1 and Model 11..... 50
Figure 46: Production performance of Models 1 through 11. 51

List of Tables

Table 1: Simulation Input for Shale Gas Reservoir with Horizontal Well..... 5
Table 2: Mid-rate Case Injection Rates 31
Table 3: Weatherford Sorption Isotherm Data..... 32
Table 4: Simulated Mid-rate Case Injection Performance for Five Samples at 4,500 psi BHP... 33
Table 5: Cumulative Injected and Adsorbed CO_2 Volumes Achieved with Different HWLs 34
Table 6: Production/Injection Effects from Varying HWLs with 600 ft Half-Wing Lengths..... 46
Table 7: Production/Injection Effects from Varying HWLs with 800 ft Half-Wing Lengths..... 46
Table 8: Production/Injection Effects from Varying Hydraulic Fracture Spacing..... 47

This page intentionally left blank.

Acronyms, Abbreviations, and Symbols

Term	Description
2-D	Two-dimensional
3-D	Three-dimensional
ARRA	American Recovery and Re-Investment Act
BHP	Bottomhole pressure
BSCF	Billion standard cubic feet
C2S2I	Carbon Capture Simulation and Storage Initiative
CH_4	Methane
CO_2	Carbon dioxide
DBD	Design Basis Document
EGR	Enhanced gas recovery
HWL	Horizontal wellbore length
ICMI	Industrial Carbon Management Initiative
MMSCF	Million standard cubic feet
MMSCFD	Million standard cubic feet per day
NETL	National Energy Technology Laboratory
OGIP	Original gas in place
PSU	Penn State University
SRV	Stimulated reservoir volume
S_W	Water saturation
WVU	West Virginia University

Acknowledgments

This work was completed as part of National Energy Technology Laboratory (NETL) research for the Department of Energy's Strategic Center for Coal as part of the Industrial Carbon Management Initiative, an American Recovery and Re-Investment Act (ARRA)-funded project. The authors wish to acknowledge Ms. Traci Rodosta (NETL Strategic Center for Coal, DOE Office of Fossil Energy) for programmatic guidance and direction; and Dr. Ronald Breault for coordinating federal research efforts on this ICMI task through the Carbon Capture Simulation and Storage Initiative project. Finally, the authors acknowledge the technical input of other university researchers for their contribution in defining and constraining the research problem, including: Professor Shahab Mohaghegh (West Virginia University (WVU), Department of Petroleum & Natural Gas Engineering); Dr. Amirmasoud Kalantari-Dahaghi (WVU, Department of Petroleum & Natural Gas Engineering); Dr. Evgeniy Myshakin (URS); Dr. Hema Siriwardane (WVU, Department of Civil and Environmental Engineering); and Mr. Christopher Jursa (URS). Finally, the authors wish to acknowledge efforts of Mr. Joel Siegel (URS) in management of ICMI Element 410 activities.

EXECUTIVE SUMMARY

The Industrial Carbon Management Initiative (ICMI) is a research project under the larger Carbon Capture Simulation and Storage Initiative (C2S2I) research program. The C2S2I has a goal of expanding the Department of Energy's (DOE) focus on carbon capture utilization and storage (CCUS) for advanced coal power systems and other applications, including the use of petroleum coke as a feedstock for the industrial sector. This American Recovery and Re-Investment Act (ARRA)-funded work supports the President's stated goal of aggressively reducing our country's energy-related greenhouse gas emissions by 8% by 2050 from a 2005 baseline. Through the ICMI project, researchers are focused on developing carbon management strategies for industrial carbon dioxide (CO_2) sources that are smaller than base-load power plants and may offer unique options for CO_2 capture, storage, or re-use. Main research thrusts in ICMI include: chemical looping technology development, carbon storage in depleted shale formations, and development/evaluation of photoactive materials to convert CO_2 to useful chemicals. While the focus of the research is industrial applications, results are expected to benefit coal power generation, as well.

In this study, the possibility of CO_2 storage in shale gas formations was investigated numerically by using an advanced computational simulator, PSU-SHALECOMP a compositional dual-porosity, dual-permeability, multiphase reservoir simulator. The simulator treated the shale gas formation as a dual-porosity, dual-permeability system consisting of shale matrix and fracture network. It is also capable of investigating the effects of water present in the micropore structure and those of matrix shrinkage and swelling in relation to CO_2 injection and production operations. In the numerical experiments considered, primarily rock and fluid properties and reservoir conditions representative of a Marcellus shale scenario were used as the basis to examine potential injection rates of CO_2 and ultimate CO_2 storage capacities in single and multiple horizontal well configurations. These configurations were located in fractured shale that has been partially depleted of natural gas through primary production.

Research objectives include the following:

- Evaluation of the potential for management of CO_2 from industrial sources through storage in depleted Marcellus shale gas wells
- Investigation of the potential to use injected CO_2 to enhance production of the remaining gas through mechanisms similar to those used in enhanced coalbed methane (CH_4) production
- Prediction of deliverability/injectivity rates that can be achieved as a function of project implementation parameters
- Investigation of CO_2 breakthrough times at production wells
- Definition and implementation of a computationally inexpensive stimulated reservoir volume (SRV) model which has the ability to generate similar behavior to that of an equivalent discrete fracture network model

The project was initiated with modification of the existing model (PSU-COALCOMP) to allow for the representation of the crushed zone (SRV) with its relevant characteristics such as inner zone fracture permeability and porosity, and matrix permeability and porosity. An SRV with gas recovery performance profiles equivalent to those predicted based on simulation of wells with

discrete hydraulic fractures was defined, and this equivalent SRV representation was used as the basis for computationally-efficient forward modeling of gas production and CO_2 storage/enhanced gas recovery (EGR) performance.

Three-dimensional (3-D) simulation runs were conducted to better represent crushed zone geometry, especially in thick shale reservoirs. In initial investigations, with an assigned net thickness of the shale at 200 ft, the SRV could be represented by an elliptical-cylinder which allows the use of two-dimensional (2-D) representation of the reservoir-hydraulic fracture-well system.

In extreme cases where gross thickness of the shale layer is approximately 2,000 ft, five layers in the z-direction were modeled to arrive at the shape of the SRV. The shape of the SRV can be represented as a cylinder (rather than an ellipsoid) with varying cylinder radii (the horizontal well being the major axis of the cylinder). The cylinder with a 600 ft radius represents the fracture half-wing penetration in every direction from the horizontal wellbore. The 1,000 ft radius represents the same, but this time for an increased SRV. With the addition of five layers in the z-direction, the size of the coefficient matrix increased along with a CPU time increase from a couple of hours to 20+ hours. Part of the research focused on methods to reduce computational time for simulation runs.

The history matching of the normalized field data was completed for 1 MMSCFD (low-rate), 10 MMSCFD (mid-rate), and 20 MMSCFD (high-rate) for initial production rates. It was shown that the PSU-SHALECOMP simulator yielded nearly perfect matches with the normalized field data when using the SRV approach. Because the SRV approach is computationally efficient as compared to discrete fraction network modeling, using this approach also allowed simulations to be completed in shorter time periods. The simulations were more stable with the SRV approach, with the model exhibiting fewer convergence problems.

2-D simulation runs were conducted to understand behavior of gas influx at different positions along the length of the horizontal well. As expected, the heel and toe ends of the well contribute to flow more than the middle segments of the horizontal well. The implication of this observation is that more stimulation around the extreme ends of the horizontal bore hole contributes to flow more extensively than other fractured stages (Vicente et al., 2002).

Preliminary results indicate that adsorption and storage of CO_2 in grid blocks around the wellbore is possible without detection of the CO_2 in neighboring production wells over a long period of injection. CO_2 breakthrough was observed in simulation results after approximately 100 years in scenarios with well spacing of 1,000 ft and no fracture connectivity between laterals. Matrix permeabilities within the nano-scale range significantly inhibit the injection of CO_2, implying that the displacement efficiency of CO_2 injection to enhance CH_4 production may be rather low in shale gas reservoirs where inter-lateral connectivity through engineered fractures is negligible.

Designs with a possible fracture hits (overlap in SRVs between adjacent fractured laterals with direct hydraulic communication) between the multi-stage fractured laterals were also investigated with a 1,000 ft well spacing. In this scenario simulations showed that injected CO_2 would be observed in the producing lateral after about 3 to 5 years as a result of possible fracture connectivity between the producer and the injector wells. This suggests that fracture connectivity between producer and injector laterals may lead to large volumes of CO_2 breakthrough early in the implementation of the CO_2 storage/ EGR project. This may indicate that CO_2 injection will

not be an economically viable alternative to displace CH_4 in cases with fracture connectivity between wells, since the fraction of CO_2 in the produced gas stream will likely require use of expensive and energy intensive CO_2/natural gas separation early in the project life.

For the range of scenarios that are considered in this study, EGR from shale by CO_2 injection is not expected to be viable. However, storage of CO_2 in depleted shale formations appears to have more promise. In the computer simulations it was observed that typically at the termination of the injection process around 10% of the injected CO_2 was found to be in the adsorbed phase and the remaining 90% in the free phase.

1. DEVELOPMENT OF THE PSU-SHALECOMP SIMULATOR

1.1 DEVELOPING CAPABILITIES OF THE RESERVOIR SIMULATOR (PSU-SHALECOMP)

Two-dimensional (2-D) validation runs for unstimulated and stimulated shale gas reservoirs were conducted using a commercial model (CMG-GEM) and the PSU-SHALECOMP simulator, a compositional dual-porosity, dual-permeability, multiphase reservoir simulator. It was verified by comparison of results that for the problems tested, both simulators are in concert.

Several sensitivity tests were also conducted to study behavior of the PSU-SHALECOMP model with application of different well types, varying horizontal borehole and fracture penetration lengths. The computer code was updated to allow runs with non-uniform fracture spacing—one of the three parameters required to define stimulated reservoir volume (SRV) in the model, along with alteration of fracture porosity and fracture permeability. Response of the model to different SRVs was studied and flow rates were compared. Additionally, 2-D simulation runs were conducted to study influx history into different segments of the horizontal well.

Various operational scenarios were studied on stimulated reservoirs. This investigation verified that horizontal wellbore length (HWL) has a significant effect on production performance, and that increase in the SRV corresponds to significant increase in total natural gas production.

1.2 COMPUTER RUNS TO STUDY THE PRODUCTION PERFORMANCE OF A REGIONAL TYPICAL SHALE GAS RESERVOIR USING PSU-SHALECOMP SIMULATOR

A series of 2-D simulator runs for unstimulated and stimulated shale gas reservoirs were performed using the PSU-SHALECOMP simulator. The main goal of these runs was to establish benchmarks to understand the performance of a typical shale gas reservoir before CO_2 injection was initiated. In designing these runs reservoir characteristics were assigned in consideration of the reported properties of the Marcellus shale formation.

In the first series of the runs, production performances of various HWLs (seven different lengths) were studied in a 405-acre drainage area for three different cases including: (1) the unstimulated reservoir conditions; (2) the case of an 18-acre stimulated area around the horizontal borehole; and (3) the case of a 36-acre stimulated area around the horizontal borehole. Table 1 provides the reservoir parameters of the given systems.

Table 1: Simulation Input for Shale Gas Reservoir with Horizontal Well

21 x 21 Simulation Input for Shale Gas Reservoir with Horizontal Well			
Depth	6,000 ft	Initial Pressure	5,000 psia
Thickness	150 ft	Sw in Fracture	0%
Area	405 acres	Sw in Matrix	0%
Fracture Porosity	1%	Langmuir Volume (CH_4)	150 scf/ton
Matrix Porosity	10%	Langmuir Pressure (CH_4)	1,281 psia
Fracture Permeability	0.001 md	Fracture Spacing	1 ft
Matrix Permeability	0.00001 md	Psf	14.9 psia
Reservoir Temperature	200°F	Wellbore Radius	0.25 ft

All of the 21 runs were designed and conducted for a total CH_4 production period of 50 years. A comprehensive production performance analysis of the runs in terms of adsorbed and free gas volumes was carried out. Significant results of this first series of runs are provided in Figures 1 through 3.

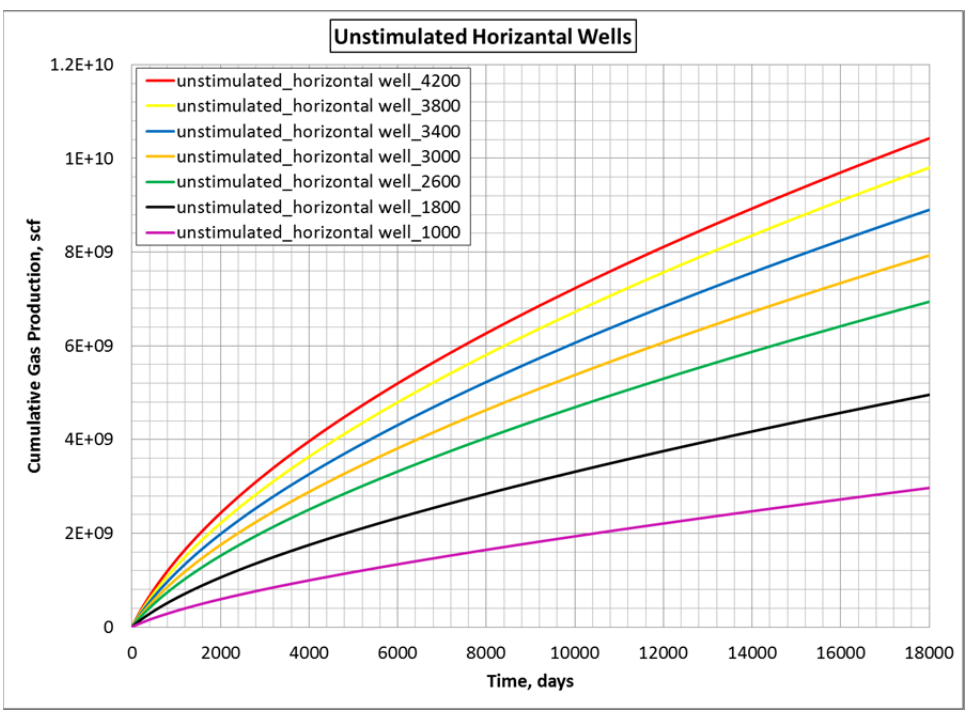

Figure 1: Cumulative production performance of unstimulated horizontal wells.

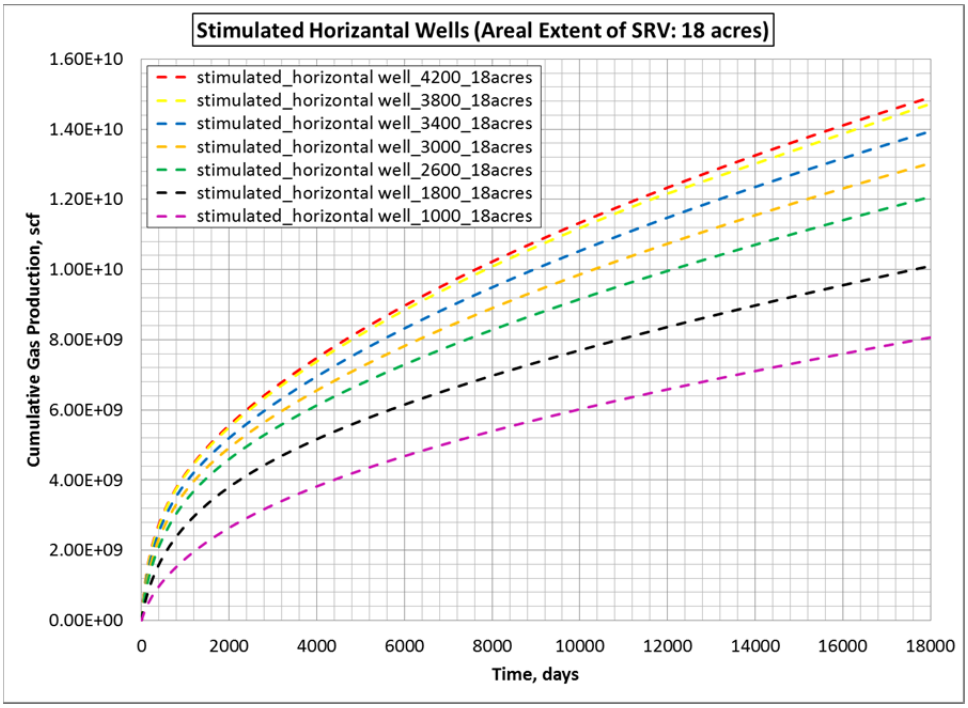

Figure 2: Cumulative production performance of stimulated horizontal wells (areal extent of SRV: 18 acres).

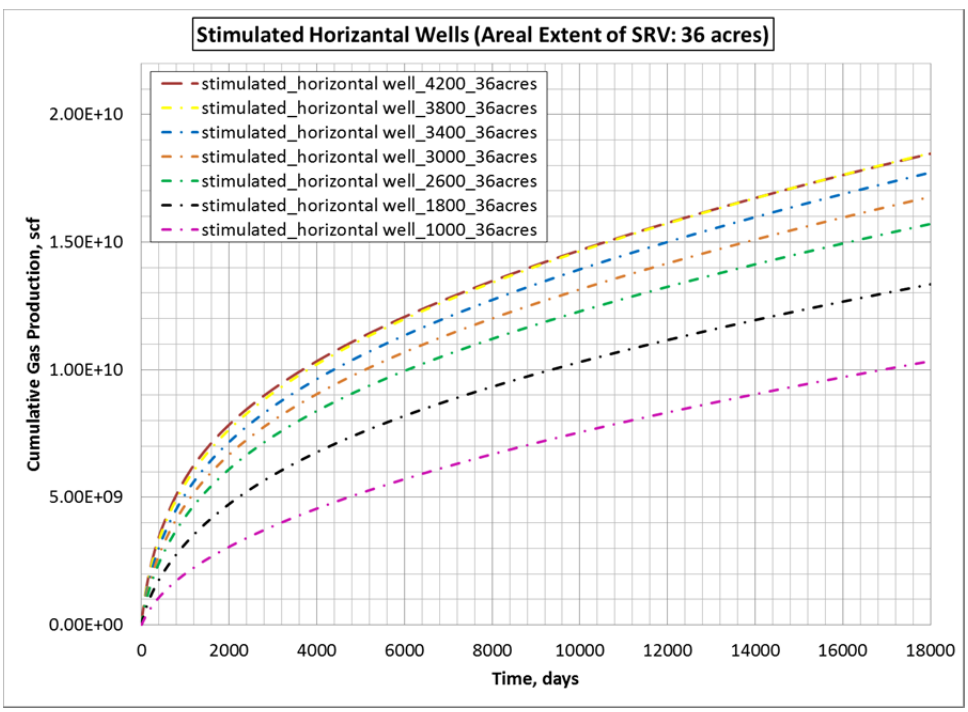

Figure 3: Cumulative production performance of stimulated horizontal wells (areal extent of SRV: 36 acres).

In the second series of simulations, another 21 runs were designed for seven different SRVs for three different HWLs. Different SRV volumes were identified based on simulation with seven minor axis lengths of the ellipses representing the SRV and three HWLs. This second series of runs was also performed for a total simulation time of 50 years. The production performances were again studied in detail in terms of adsorbed and free gas volumes of each system. Significant results observed in this second series of runs are provided in Figures 4 through 6.

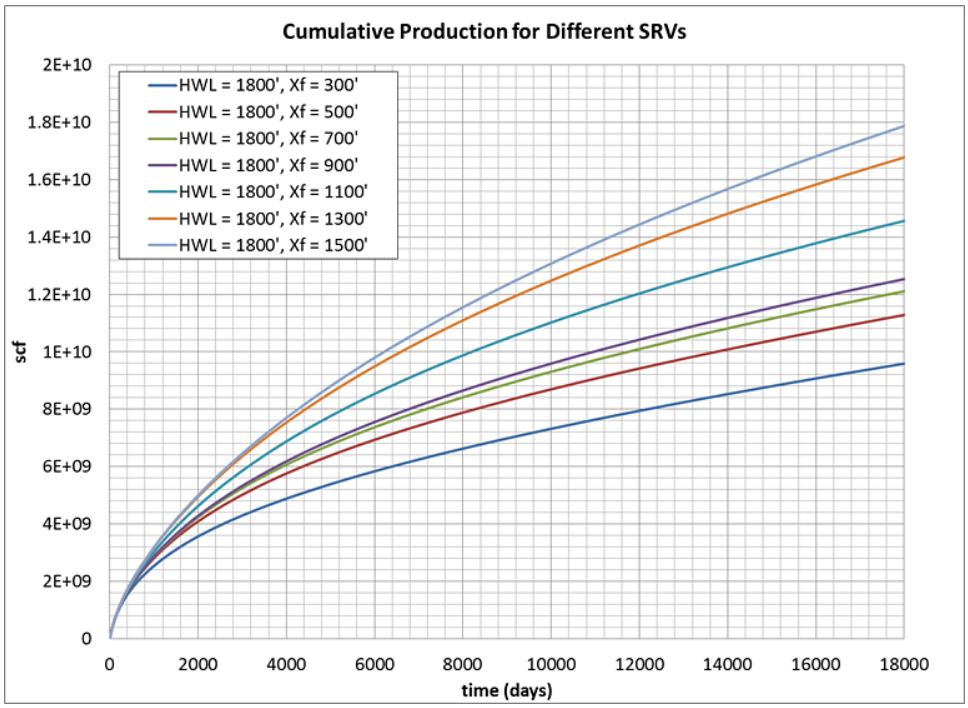

Figure 4: Cumulative production performance of different SRVs (HWL = 1,800 ft).

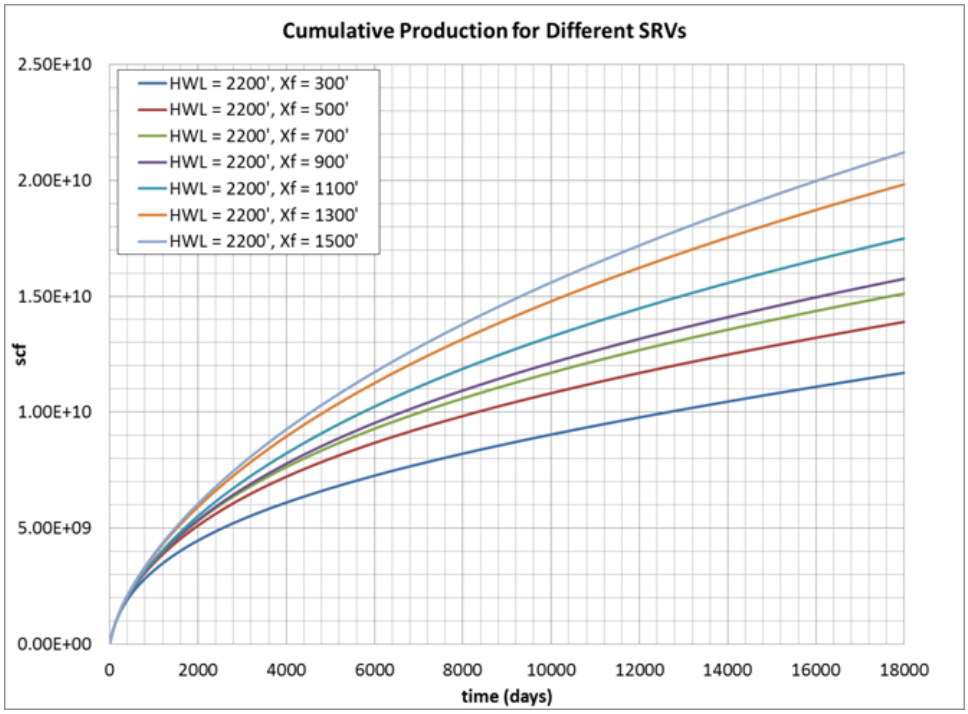

Figure 5: Cumulative production performance of different SRVs (HWL = 2,200 ft).

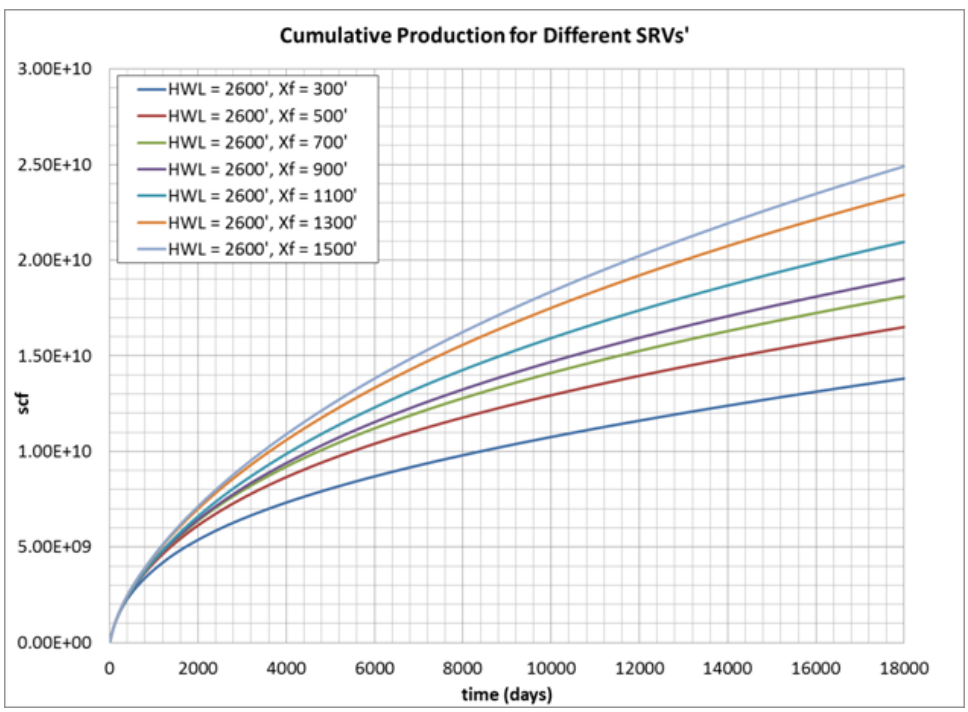

Figure 6: Cumulative production performance of different SRVs (HWL = 2,600 ft).

As long as drainage area for the short and long laterals is the same, then the extent of the SRV zone plays a more significant role in ultimate recovery than the HWL.

Additionally, if a shale reservoir is stimulated, a well produces at high rates in the early phase of the production which reduces the reservoir pressure earlier than the unstimulated case. Once the boundary effects are felt, the production rate decreases sharply (Figure 7).

The reservoir pressure in unstimulated models supports the production in the later phases. However, it can be seen that the cumulative production curves are rather linear in the unstimulated case (Figure 8). Boundary effects come into the picture in later phases for the unstimulated cases. Since, the simulation run time is 50 years, unstimulated cases can get closer values to the stimulated cases at the end of the simulations. However, in early to middle times cumulative production is much larger in the stimulated cases.

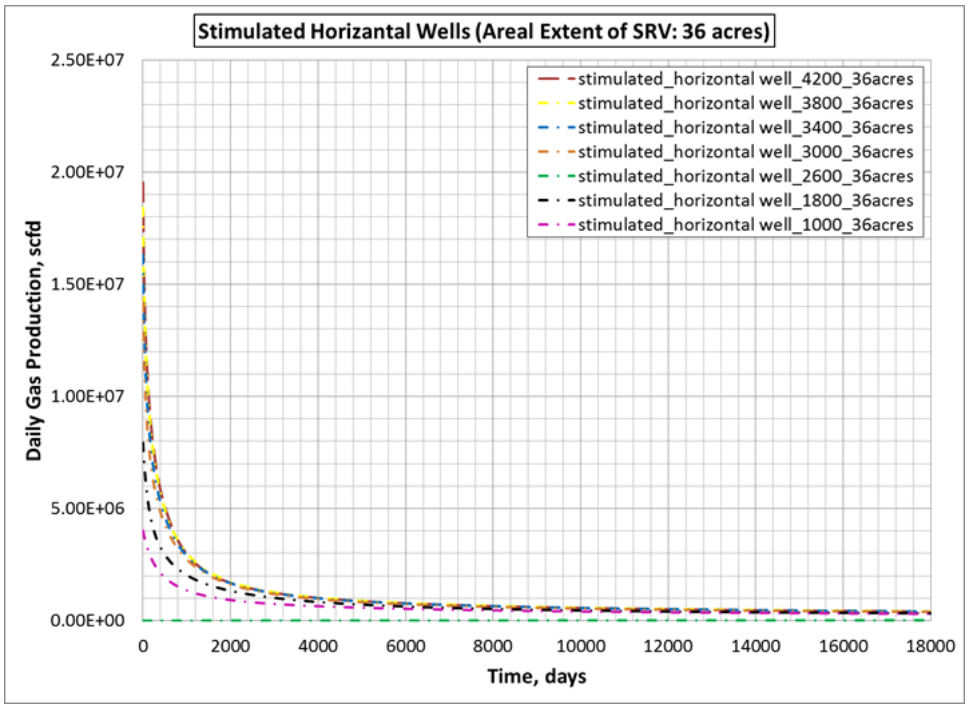

Figure 7: Daily gas production for stimulated wells.

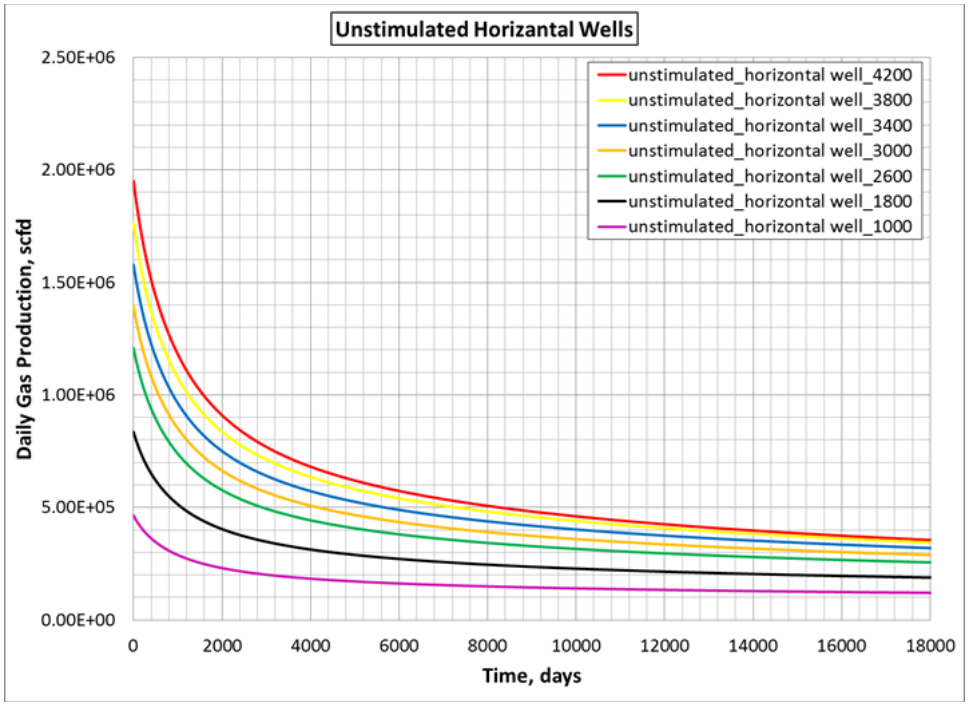

Figure 8: Daily gas production for unstimulated wells.

1.3 DESIGNING PRELIMINARY RUNS INVOLVING CO_2 INJECTION

An additional series of 2-D simulation runs was carried out to characterize the flow dynamics of CO_2 injection in shale gas reservoirs. The PSU-SHALECOMP model was tested in a single-processor environment and large run times were observed (10 years of simulation taking almost one week for a 21 x 21grid system). The principal goal of these simulation runs was to establish some benchmarks to understand the performance of a shale gas reservoir during CO_2 injection. Four different simulation studies were considered:

- Simulation 1: all wells produce natural gas for 50 years
- Simulation 2: all wells produce natural gas for 30 years, followed by 20 years of CO_2 injection into corner wells
- Simulation 3: all wells produce natural gas for 20 years, followed by 30 years of CO_2 injection into corner wells
- Simulation 4: CO_2 is injected into all wells before any natural gas production (from Year 0) until injection maximum pressure is reached (assumed to be 8,000 psi)

In designing these runs, reservoir characteristics were assigned in consideration of the reported properties of the Marcellus shale formation as summarized in Figure 9. Results of these runs are presented in terms of production profiles, pressure distributions over the reservoir, and CO_2 mole fraction distributions in the adsorbed and free phases across the reservoir.

Performance of the PSU-SHALECOMP in these two-component compositional runs was found to be satisfactory.

Figure 9 shows the reservoir parameters and the wellbore pattern design for CO_2 injection simulations.

7x7 Simulation Input for Shale Gas Reservoir with Horizontal Wells			
Depth	6,000 ft	Langmuir Pressure (CH_4)	1,281 psi
Thickness	150 ft	Langmuir Volume (CO_2)	774 scf/ton
Area	405 acres	Langmuir Pressure (CO_2)	276 psi
Fracture Porosity	1%	Fracture Spacing	1 ft
Matrix Porosity	10%	P_{sf}	14.9 psi
Fracture Permeability	0.001 md	HW Length (Center)	3,000 ft
Matrix Permeability	0.0001 md	HW Length (Corners)	1,200 ft
Reservoir Temperature	200°F	Fracture Wing	900 ft
Average Pressure	5,000 psi	Fracture Porosity	2%
S_w in Fracture	0.01%	Fracture Permeability	0.01 md
S_w in Matrix	0.01%	Fracture Spacing	0.1 ft
Langmuir Volume (CH_4)	150 scf/ton		

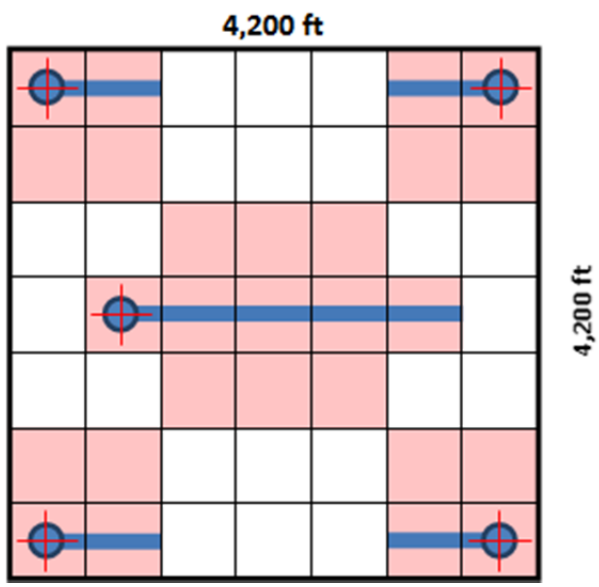

Figure 9: Scenario definition used in CO_2 injection sensitivity simulations: parameter values and model well pattern configuration.

While this well pattern configuration is not representative of real world configurations, it serves as a useful model case to explore performance of adjacent lateral interaction and importance of offset distance on fluid migration and pressure response. This configuration was studied to understand the degree of interactions between injectors and producers using a five-spot pattern with four injectors at the corner and one producer at the center of the configuration.

Figures 10 through 13 display the production performances of the four cases studied.

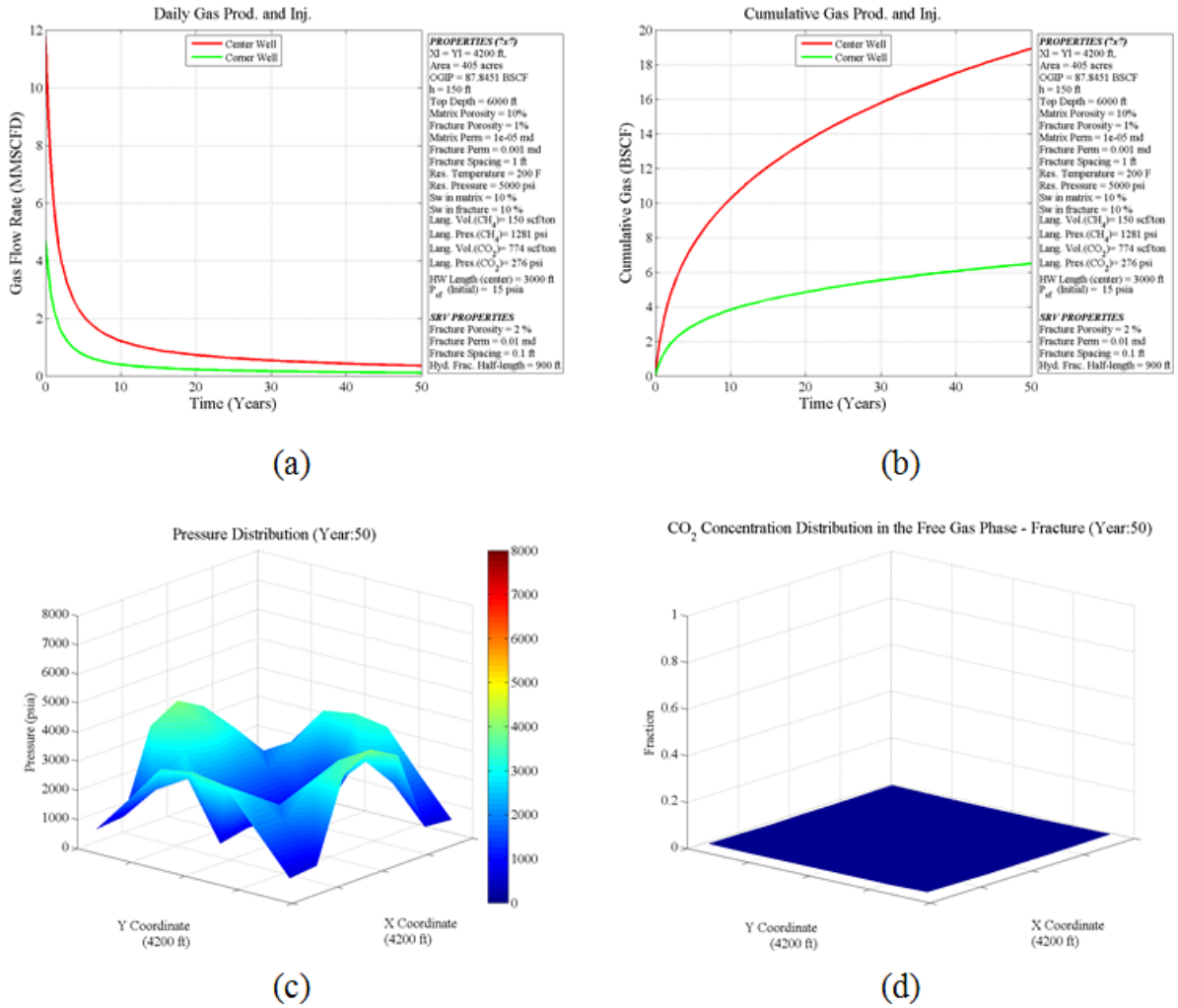

Figure 10: Simulation 1: (a) daily production rate, (b) cumulative production, (c) final pressure distribution, and (d) final CO_2 concentration distribution.

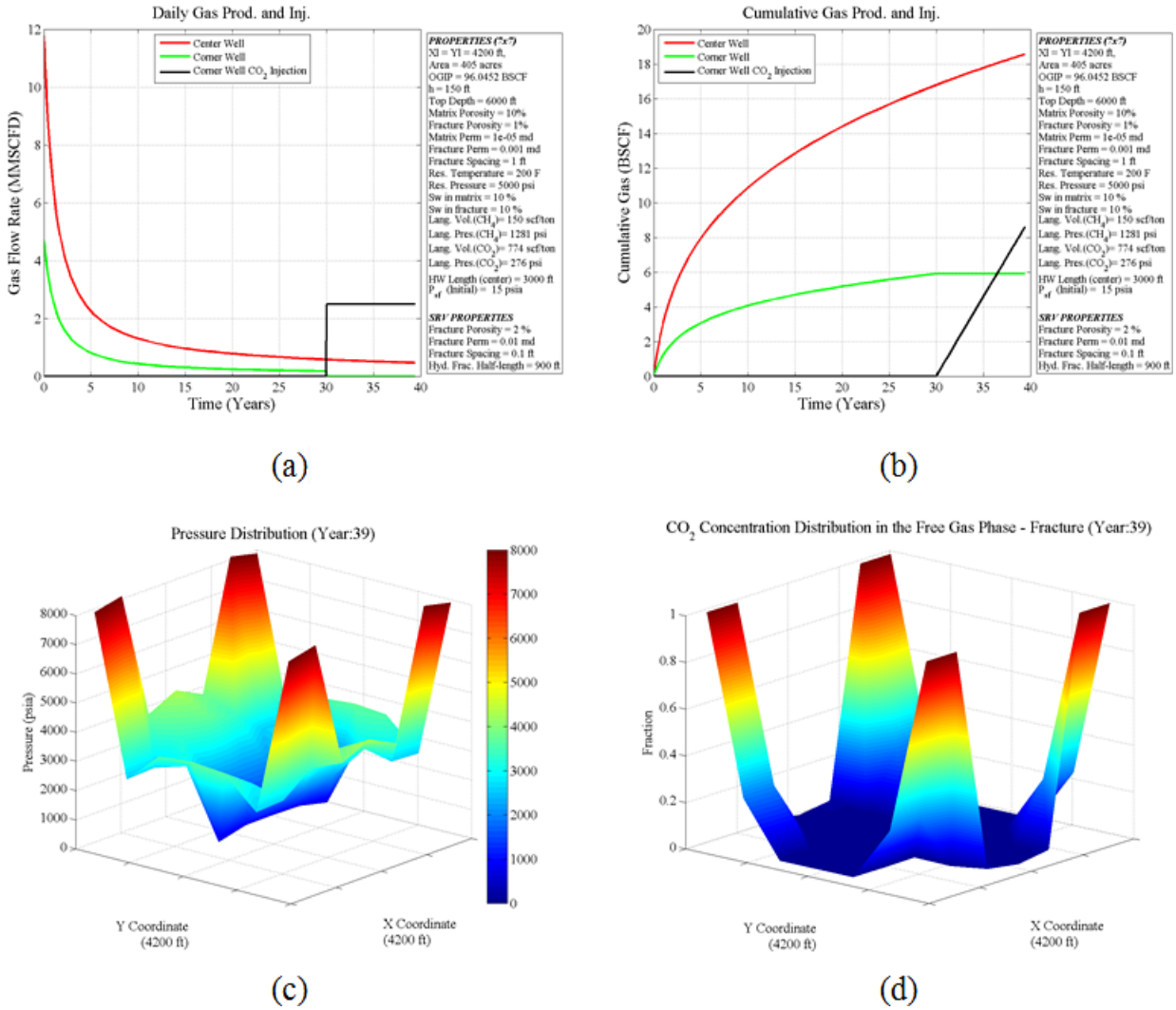

Figure 11: Simulation 2: (a) daily production rate, (b) cumulative production, (c) final pressure distribution, and (d) final CO_2 concentration distribution.

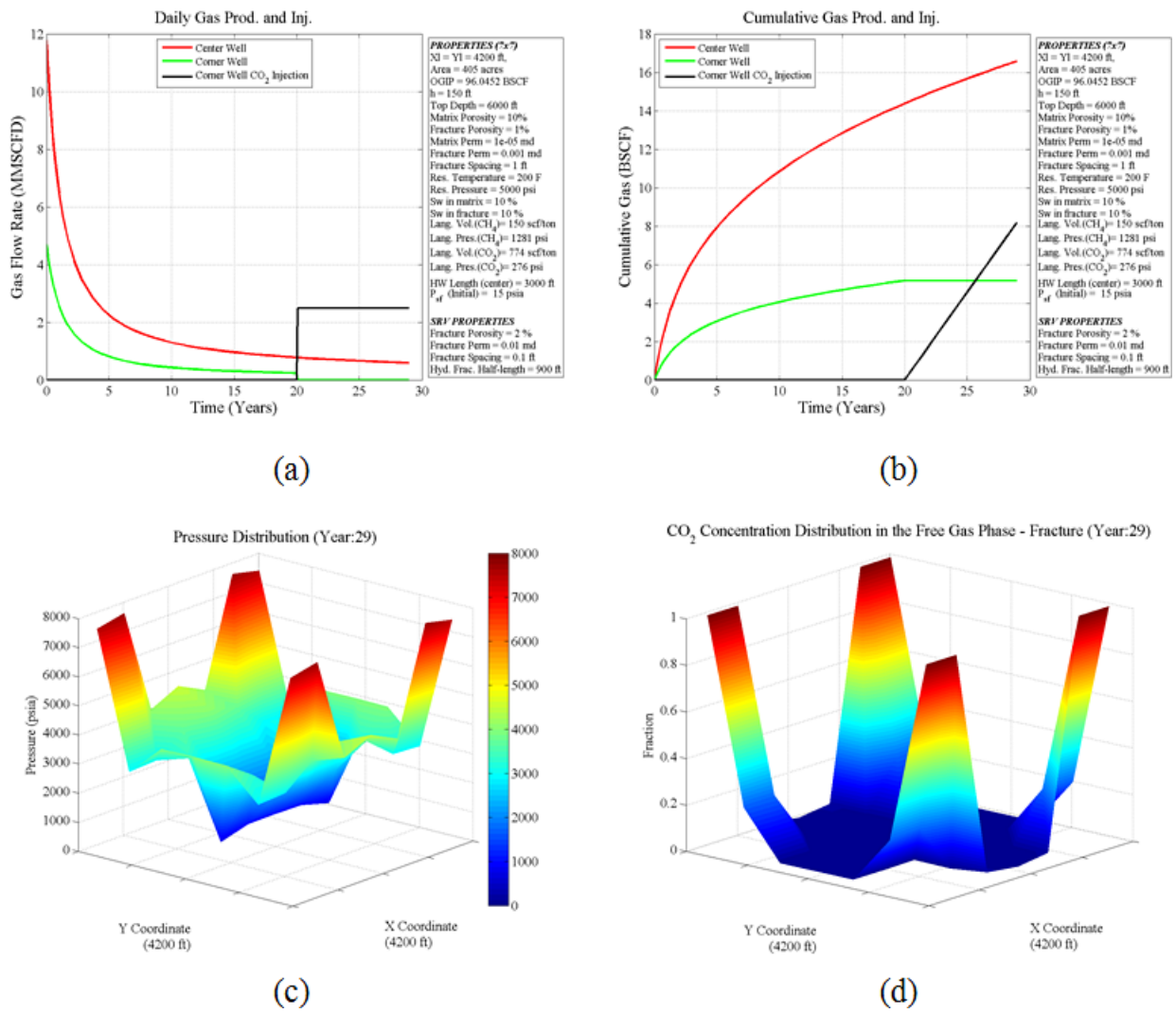

Figure 12: Simulation 3: (a) daily production rate, (b) cumulative production, (c) final pressure distribution, and (d) final CO_2 concentration distribution.

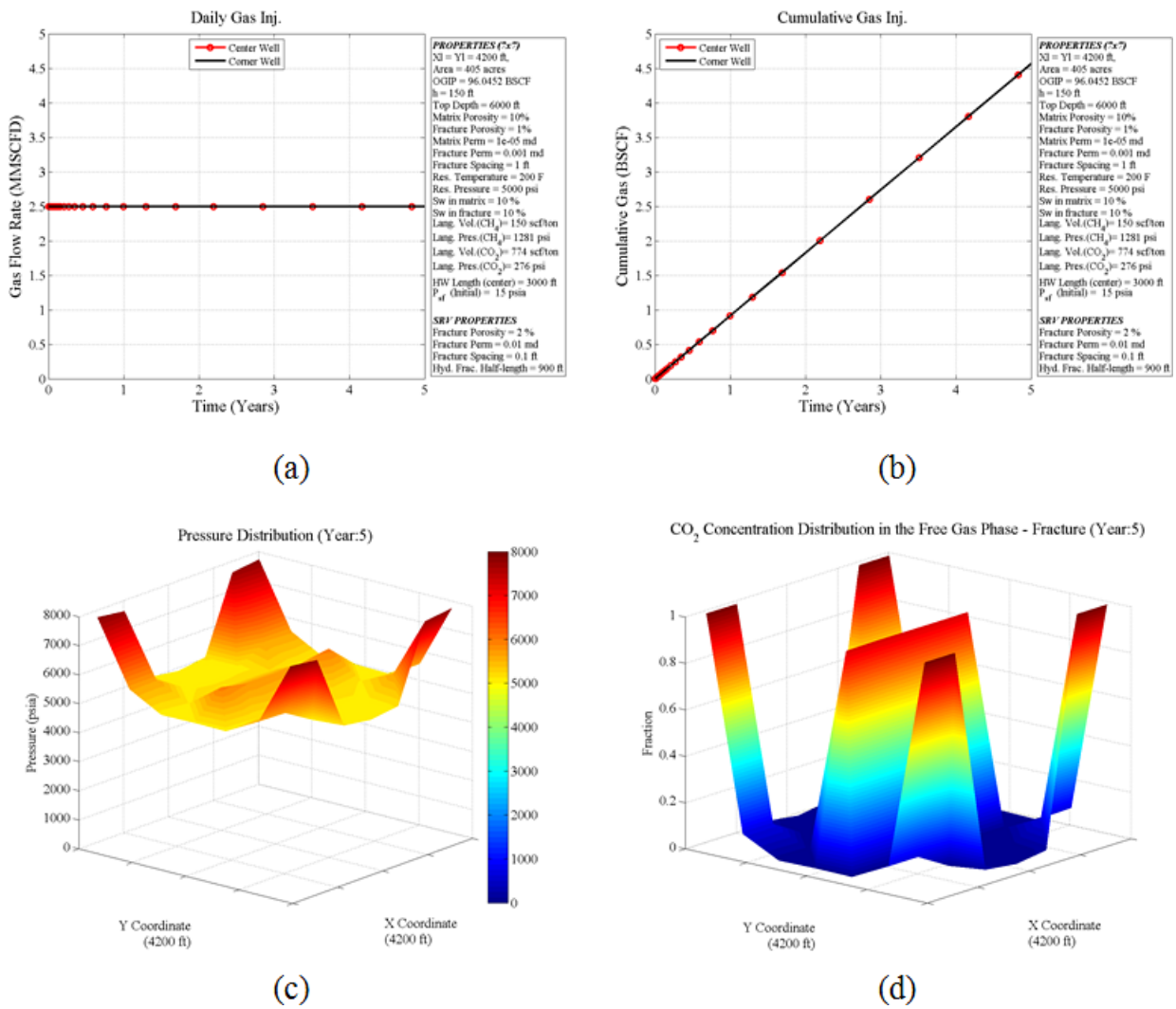

Figure 13: Simulation 4: (a) daily production rate, (b) cumulative production, (c) final pressure distribution, and (d) final CO_2 concentration distribution.

Preliminary results of these CO_2 injection simulations indicate that adsorption and storage of CO_2 in grids around the wellbore is possible without CO_2 breakthrough to neighboring production wells over long periods of injection times.

It was observed that matrix and natural fracture permeability values will control the distribution of the injected CO_2, and that formation thickness and shale adsorption characteristics (Langmuir volume and Langmuir pressure values) control the amount of CO_2 stored. However, matrix permeabilities within the nano-scale strictly block the injection of CO_2.

1.4 WELL-SPACING/PATTERN OPTIONS STUDIED TO UNDERSTAND THE CO_2 FLOW BEHAVIOR IN NANODARCY SHALE FORMATIONS

Comparison of simulated performance of CO_2 injection into shale gas reservoirs was made using two independently developed models: CMG-GEM and PSU-SHALECOMP. Comparison was made based on properties prescribed in the ICMI Design Basis Document (DBD) common design problem. The results indicate that both simulators produced similar pressure distribution patterns as shown in Figure 14. In the absence of real data on formation response to CO_2 injection, model comparison results offer the best available means of developing confidence in performance of PSU-SHALECOMP.

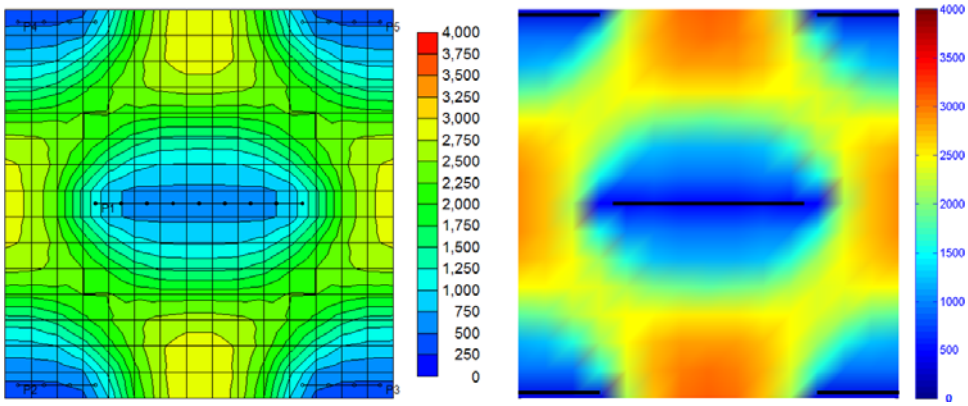

Figure 14: Pressure distributions of CMG (left) and PSU-SHALECOMP (right) at year 30.

Different well-spacing/pattern options were studied to understand the CO_2 flow behavior in nanodarcy shale formations. Preliminary results show that the depleted shale reservoirs are good candidates for CO_2 storage. Depending on the well spacing and the extent and the transport characteristics of the SRV, it is observed that the CO_2 breakthrough time will be extensively longer in shale formations as compared to deep coalbed reservoirs.

The molar concentrations of CH_4 in well blocks were very close to 1 due to CO_2 injection. Therefore, the previous generation solver routine was unable to solve matrix equations generated (because of the ill conditioned nature of the Jacobian matrices, where ill conditioned refers to cases with high condition number - absolute value of the asymptotic worst case relative change in output resulting from a relative change in input). With the incorporation of a new solver routine, this issue was resolved.

1.5 SIMULATIONS WITH DIFFERENT WELL PATTERNS WITH POSSIBLE FRACTURE ('FRAC') HITS TO THE NEIGHBORING WELLS

Production Performance of Tight Shale Systems

After development of the SRV approach, preliminary assessment of CO_2 injectivity in a model well pattern configuration, and developing confidence in CO_2/shale simulation by inter-model comparison, research focus shifted to evaluation of a more realistic scenario of injector/producer operational paradigm in adjacent, parallel multi-stage laterals.

In the previous well pattern simulations (Section 1.3) CO_2 breakthrough was seen only after 100 years of injection with no fracture hit. Matrix permeabilities within the nano-scale range

effectively blocked the injection of CO_2. Designs with possible frac hits (the intersection of two SRV zones originating from two different laterals) were investigated with 1,000 ft of well spacing. CO_2 was observed within 3 to 5 years at the producer if there was a potential frac hit between the producer and the CO_2 injector.

Simulations with potential frac hits provide three insights:

1. CO_2 breaks through quickly to the production well in cases with a frac hit
2. CO_2 takes the "path of least resistance" and so does not significantly contact the matrix to enhance gas recovery (the residence time at a given location should not be significantly less than the adsorption time constant)
3. Injecting CO_2 later in the gas production life of the pad reduces enhanced gas recovery (EGR) potential

CO_2 injection ***does not contribute*** to a significant increase in CH_4 production if there is a frac hit between the injector and the producer laterals, and frac hits lead to large amounts of CO_2 breakthrough. Simulations also indicated that displacement efficiency of CO_2 injection to enhance CH_4 production is rather low. In order to realize more pronounced EGR, it will be necessary to start injection early in the life of a project. Figures 15 through 18 show multiple cases with differing well patterns.

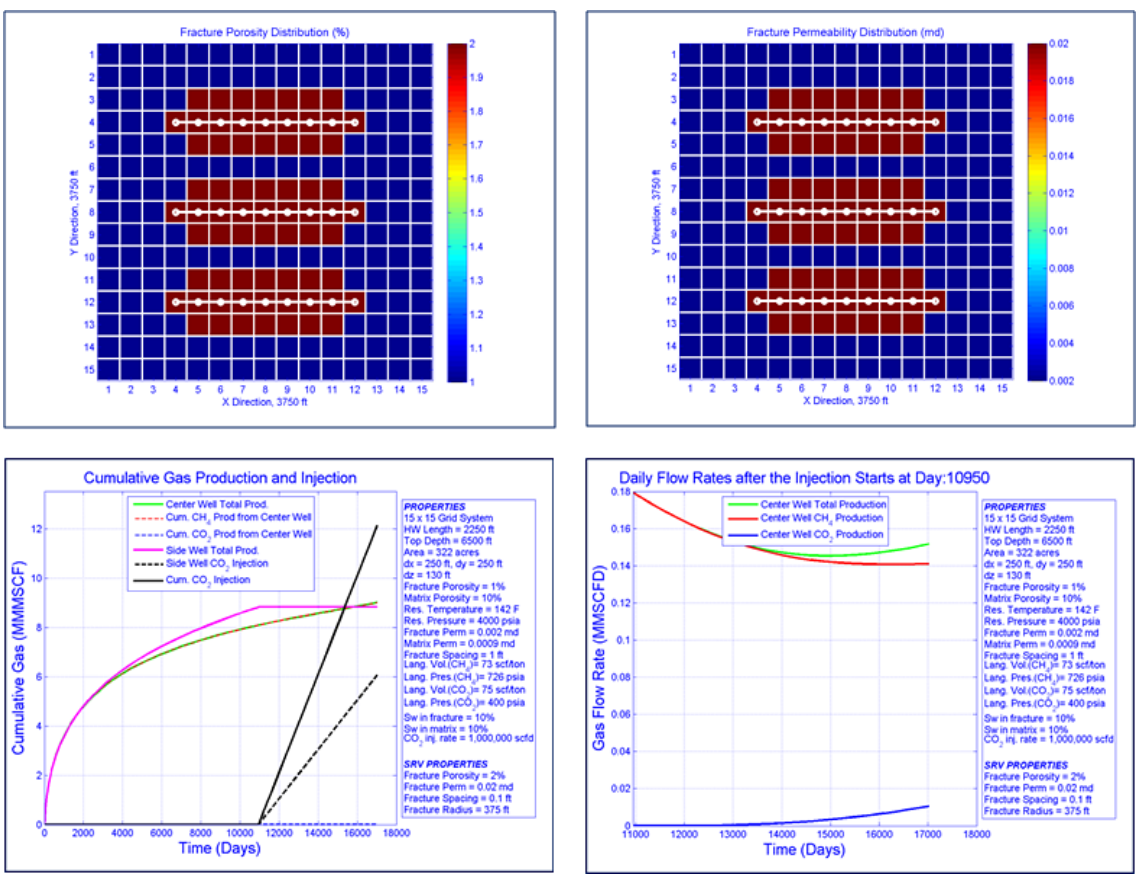

Figure 15: Case 1, CO_2 production investigation at the center well (connectivity between the wells exists).

For Case 1, the chart on the right bottom shows the injection period, which started after 30 years of production (Figure 15). The side wells are converted to injectors and the center well keeps producing to investigate CO_2 production. It can be seen that a small amount of CO_2 production is observed after 8 years of injection at the center well. Furthermore, CH_4 production at the center well is not enhanced significantly (due to CO_2 injection).

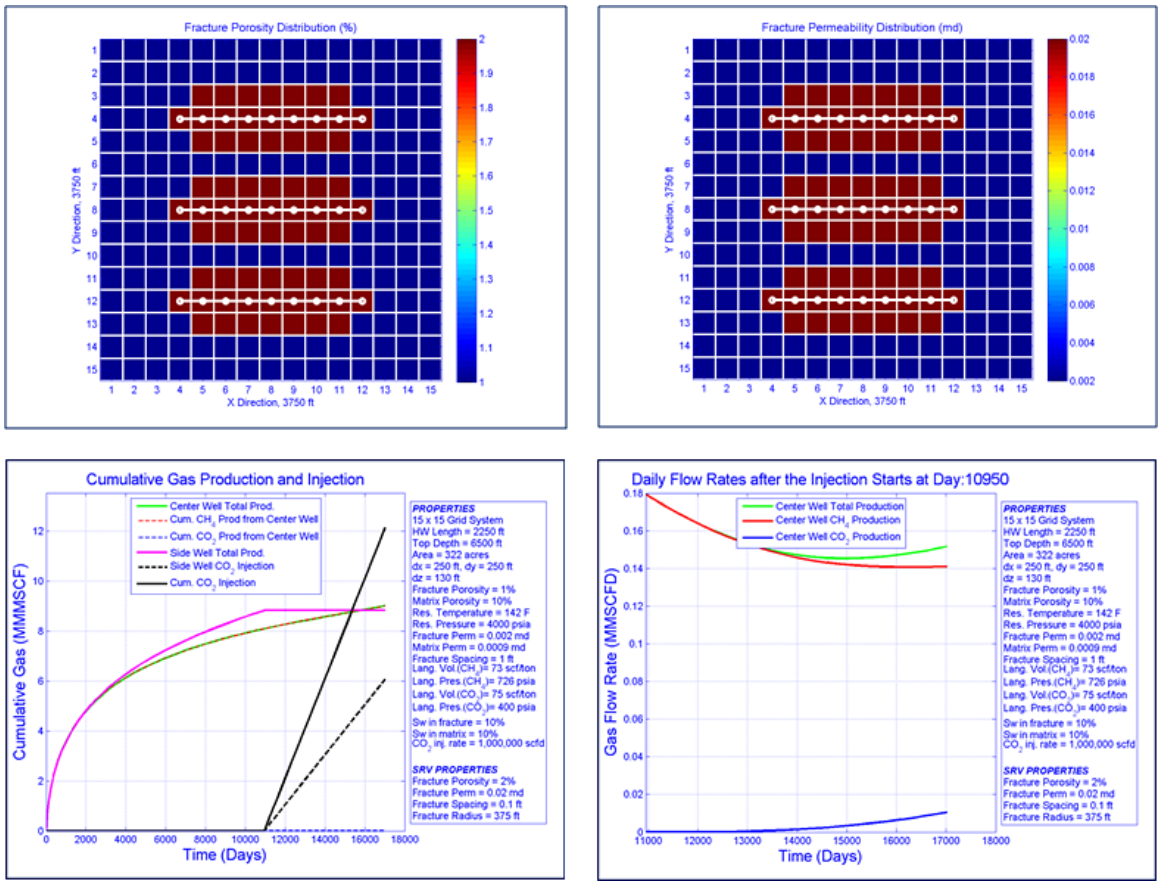

Figure 16: Case 2, CO_2 production investigation at the center well (connectivity between the wells does not exist).

There is a small amount of CO_2 production observed at the center well after 8 years for Case 2 (Figure 16). The daily CO_2 flow rate curve shows much smaller profiles as compared to Case 1. This shows that enhancing CH_4 production by injecting CO_2 does not have an impact since the formation is very tight.

Production Performance of More Permeable Shale Systems

Since the systems studied in Cases 3 and 4 are more permeable than the previous cases investigated (1 and 2), CO_2 breakthrough at the producer is seen sooner.

In Case 3 (Figure 17), the reservoir system is more permeable and there is connectivity between the wells due to hydraulic fracturing, CO_2 production is encountered in a short period of time (small residence time for CO_2 injected).

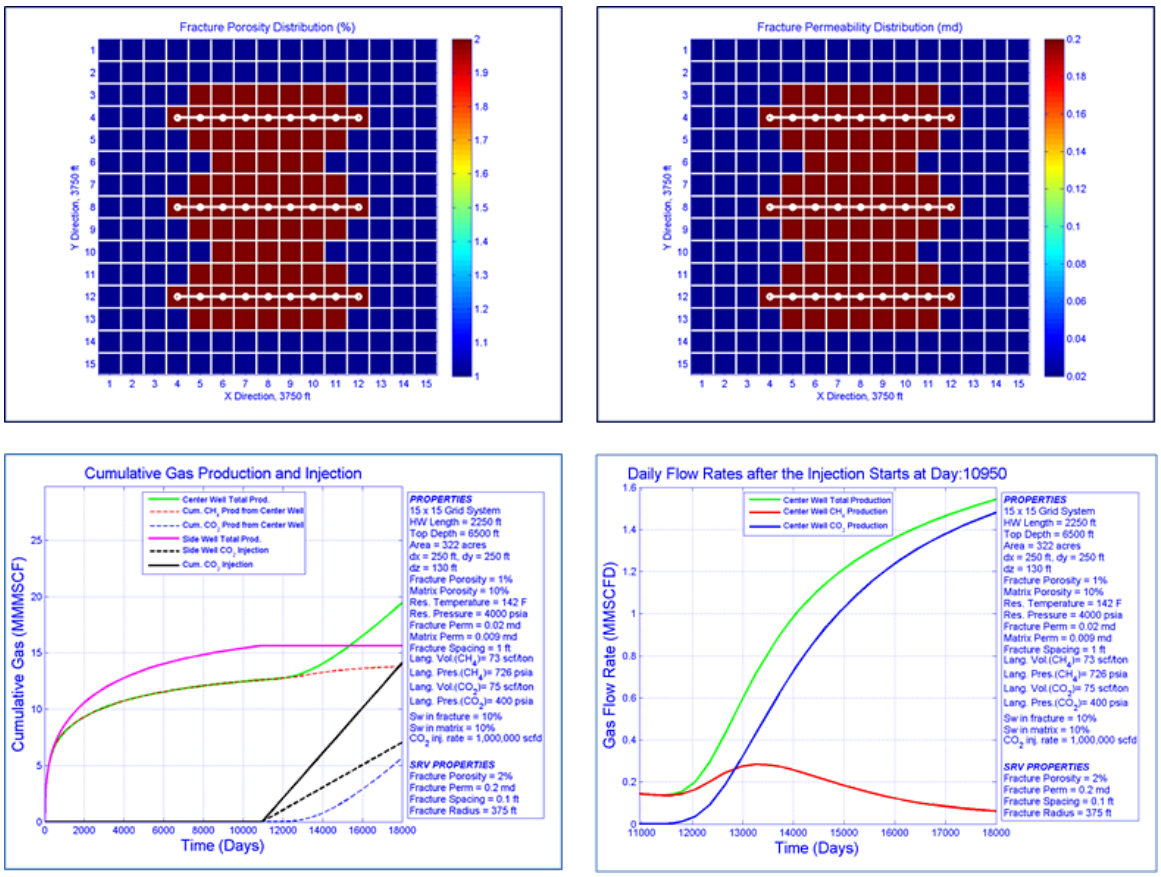

Figure 17: Case 3, CO_2 production investigation at the center well (connectivity between the wells exists).

A relatively small increment of CH_4 production is observed due to CO_2 injection. Not only will injection of CO_2 not have a significant contribution to CH_4 production and EGR, the CO_2 in the produced CH_4 stream will have to be separated. This can be observed in Figure 17 (bottom-right chart). The red line shows that there is a small increment in CH_4 production. Also, CO_2 production is encountered at the center well about the third year of injection from the side wells, which is about the 11,800th day.

Figure 18 shows the top view of Case 4. It can be seen that there is 250 ft distance between the stimulated reservoir volumes.

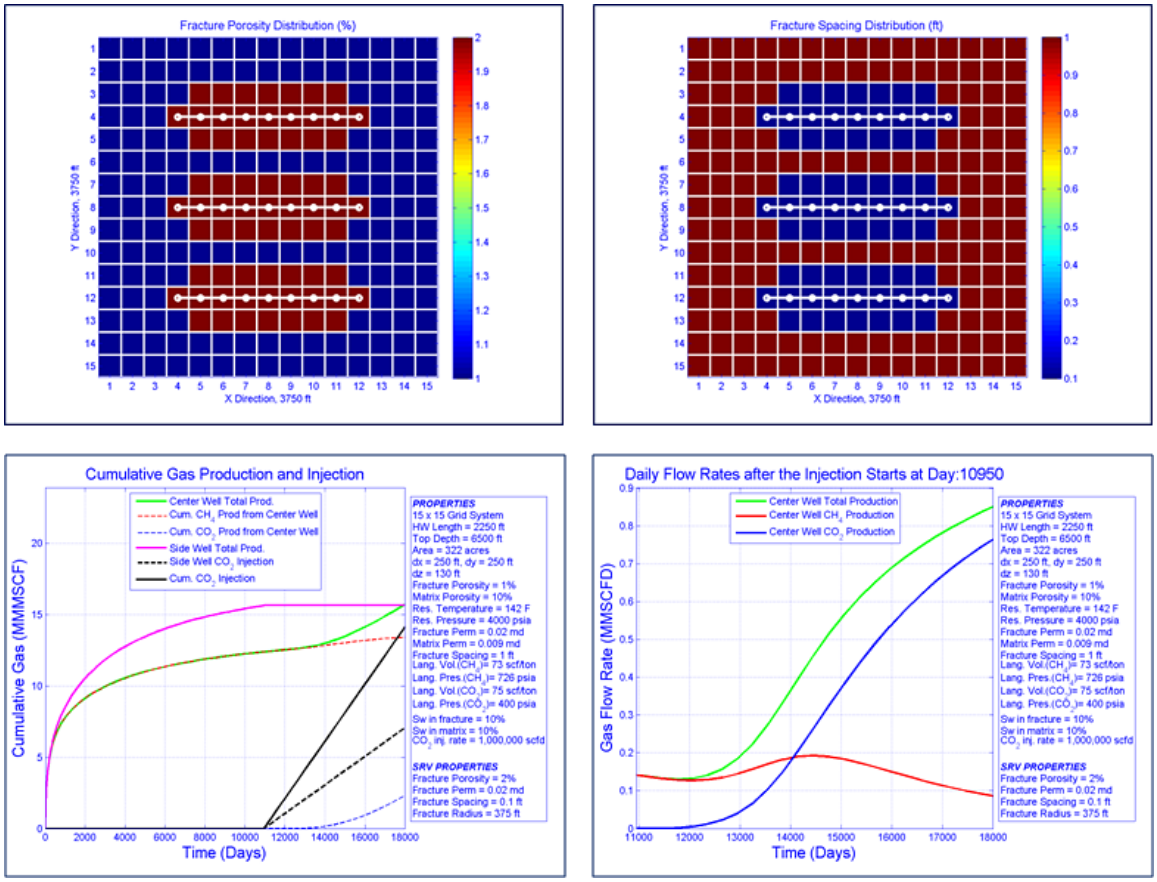

Figure 18: Case 4, CO_2 production investigation at the center well (connectivity between the wells does not exist).

CO_2 production is seen later and in much smaller quantities. Cumulative CH_4 production values are almost the same for Cases 3 and 4. However, the total CO_2 production in Case 4 is less more than half the CO_2 production in Case 3.

An important insight from simulation efforts is that very little fluid injectivity into ultratight systems such as shale formations is expected, unless extensive stimulation around the injectors is achieved. As a result, only small incremental CH_4 production is observed as a result of CO_2 injection.

Due to favorable Langmuir Volume and Langmuir Pressure constants of CO_2 as applicable to shale formations and the potential of encountering large reservoir thicknesses, it is still viable to inject large volumes of CO_2 without exceeding the physical limits of the injection pressure.

Simulations with smaller well spacing were also investigated as the distance between the neighboring wells has a big impact on CO_2 injection and also on its production. Some new injection applications including cyclic injection patterns, as well as injection patterns accommodating infill injector options, should be considered in future studies.

2. HISTORY MATCHING OF NORMALIZED FIELD DATA

History matching of the normalized field data was completed for 1 MMSCFD (low-rate), 10 MMSCFD (mid-rate), and 20 MMSCFD (high-rate) initial production rates. The PSU-SHALECOMP simulator yielded near-perfect matches compared to the normalized field data, provided by Dr. Mohaghegh's team at West Virginia University (WVU), when implementing the SRV technique. For the low-rate case, the minimum characteristic values for the parameters are used as provided in Tables 3-2 and 3-3 of the ICMI DBD (Appendix A). Similarly, mean values are used for the mid-rate case and maximum values are used for the high-rate case. The data used is summarized in Figure 19.

In shale gas reservoirs, sharp production declines in the late stages are usually not observed. This is attributed to well-known rate transient characteristic of shale reservoirs in which boundary dominated flow does not apply. Accordingly hyperbolic decline curves are expected to represent shale production performances of shale gas reservoirs more effectively than exponential decline curves. Shale gas wells are capable of producing CH_4 feasibly more than 20 years.

An additional peripheral study was conducted for Dr. Blumsack's team about industrial CO_2 delivery to wellheads and its injection. Actual CO_2 data that is produced via industrial facilities as provided by Dr. Blumsack's team were used in these simulations.

Simulation Data			
Parameter	Low-	Mid-	High-
Production Rate (MMSCF)	1	10	20
Grid System	17x17	17x17	17x17
Grid Size on X Direction (ft)	100	215	270
Grid Size on Y Direction (ft)	80	215	270
Area (acres)	53	307	484
Thickness (ft)	264	271	276
Depth (ft)	6,500	6,500	6,500
Matrix Porosity (%)	6	8.5	11
Fracture Porosity (%)	0.6	1.05	1.5
Matrix Permeability (md)	0.0003	0.0006	0.0009
Fracture Permeability (md)	0.0007	0.00185	0.003
Fracture Spacing (ft)	2.5	1.7	0.9
Reservoir Temperature (°F)	142	142	142
Reservoir Pressure (psi)	3,940	3,940	3,940
S_w in Matrix (%)	10	10	10
S_w in Fracture (%)	10	10	10
Langmuir Volume of CH_4	73	73	73
Langmuir Pressure of CH_4 (psi)	726	726	726
Langmuir Volume of CO_2	75	75	75
Langmuir Pressure of CO_2 (psi)	400	400	400
Horizontal Wellbore length (ft)	500	1,935	2,970
Hydraulic Fracture Half-length	120	537.5	675
P_{sf} (psi)	568	495	1,110
SRV Fracture Porosity (%)	1.2	2.1	3
SRV Fracture Perm (md)	0.007	0.0185	0.03
SRV Fracture Spacing (ft)	0.25	0.17	0.1

S_w	K_{rw}	P_{cow}
0	0	0
1	0	0

S_g	K_{rg}	P_{cog}
0	0	0
1	1	0

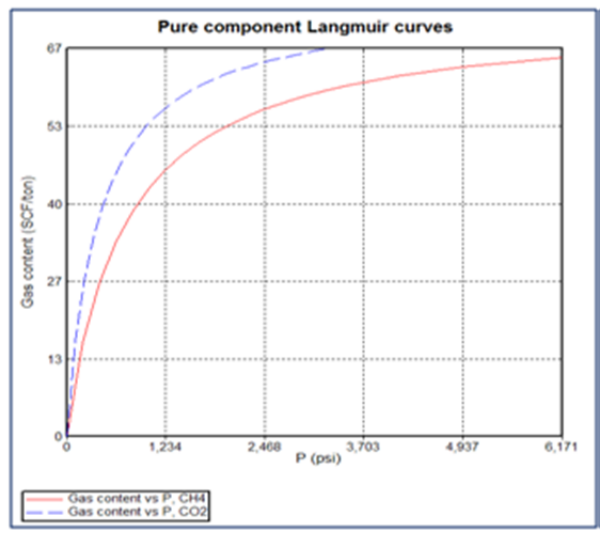

Figure 19: Data used for low-rate, mid-rate, and high-rate simulations.

2.1 LOW-RATE CASE INITIAL PRODUCTION

In this history match, the reservoir area had to be kept relatively small, as well as the HWL and hydraulic fracture dimensions, in order to match the proposed initial flow rate, which is 1 MMSCFD, to show the performance of the model in a low-productivity system. The importance of HWLs and hydraulic fracture dimensions is heightened when low production values are encountered during the production stage. In this case, the model uses extreme low values of the dataset in the DBD. With relatively small HWLs and hydraulic fracture dimensions, CH_4 production becomes rather unfeasible. Moreover, cumulative CO_2 injection volumes do not reach desirable high volumes because of high pressures at the injection well block.

Figure 20 shows the daily flow rate and the cumulative production of CH_4 vs. time.

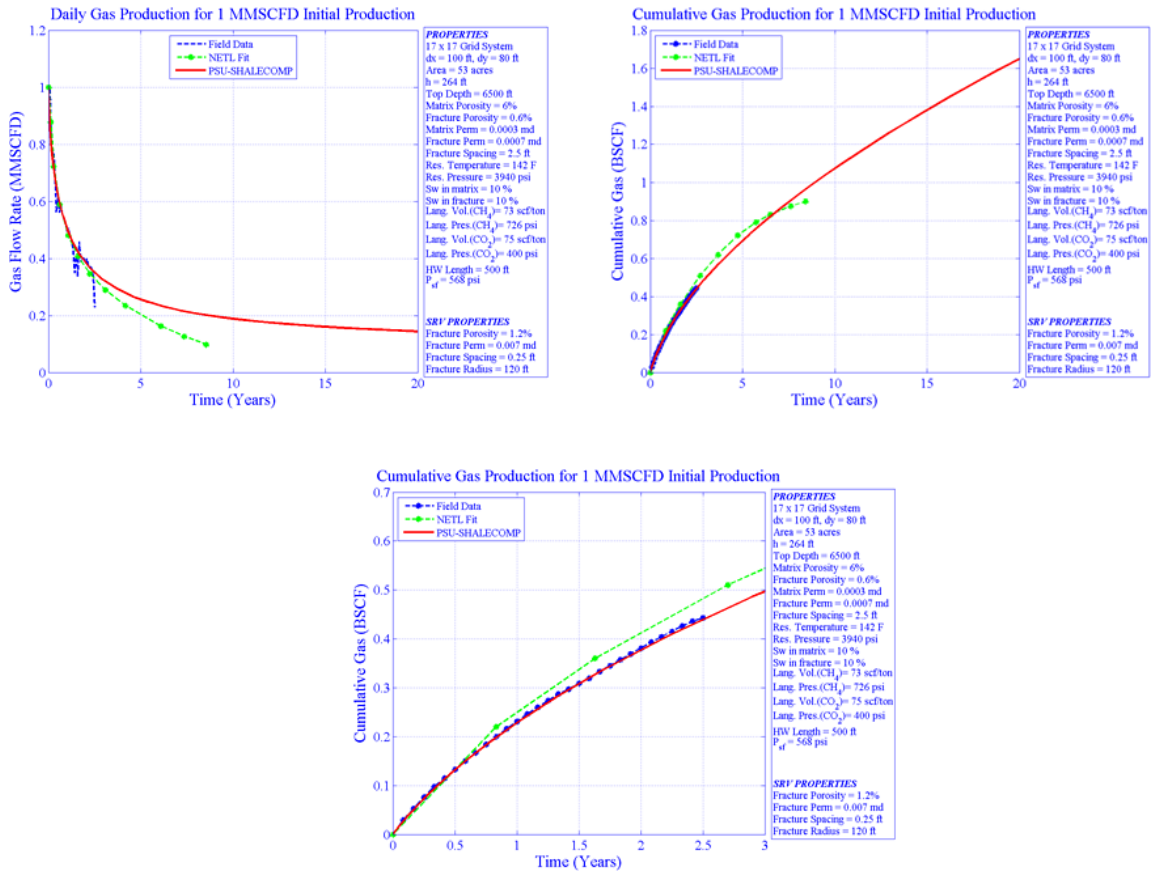

Figure 20: Low-rate case history match.

Also, CO_2 injection possibilities were investigated for the low-rate case. At the end of the 3rd year of injection, simulation was stopped because of the pressure constraints at the well blocks since they had reached 7,000 psi (Figure 21). These high pressures may induce unwanted fractures of environmental concern (i.e., connect the shale formation to the overburden and/or overburden formations). Cumulative CO_2 injection volumes do not reach desirably high volumes which will make the project increasingly more feasible, because of high pressures at the injection well block. Thus, controlled injection of CO_2 into that particular formation may prove to be infeasible.

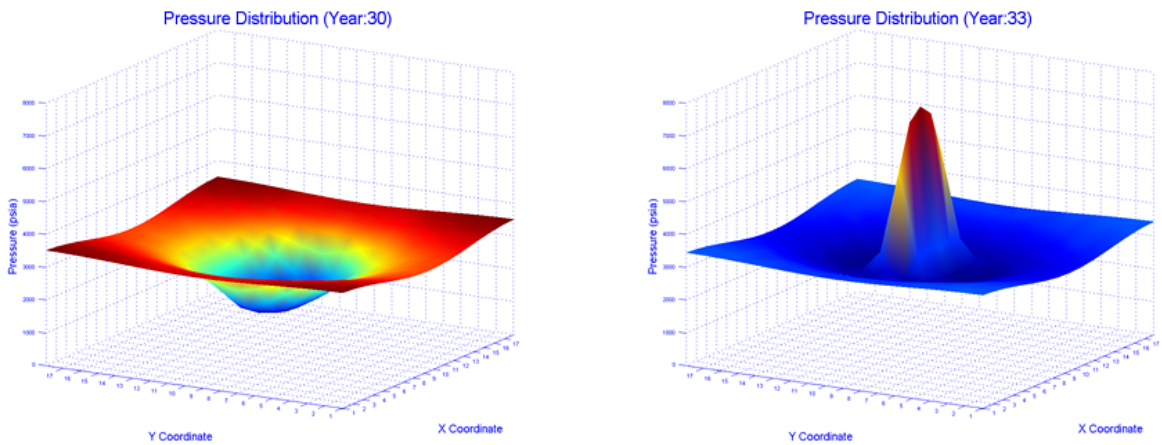

Figure 21: Low-rate case pressure distribution.

2.2 MID-RATE CASE INITIAL PRODUCTION

In this history match, the reservoir area was determined to be 307 acres. HWL and hydraulic fracture dimensions were adjusted to match the proposed initial production rate as 10 MMSCFD. Figure 22 shows the daily flow rate and the cumulative production of CH_4 vs. time. The PSU-SHALECOMP's results have near perfect fit with the normalized field data with the implementation of the SRV concept.

CO_2 injection possibilities were investigated for the mid-rate case. Since the reservoir is almost 6 times larger than the reservoir of the low-rate case, well-block pressures (Figure 23) reach high values after a much longer period of injection (15 years of injection was accomplished in this application).

The drainage area assigned in this model is rather large as a pattern area. It can be observed that the well produces almost 1 MMSFCD at the 30th year, which makes it still economical. The cumulative production (Figure 24) indicates that there is 17 BSCF of total CH_4 production and 8.3 BSCF of CO_2 injected.

Mid-rate case values used as reservoir input parameters, were derived from the DBD document.

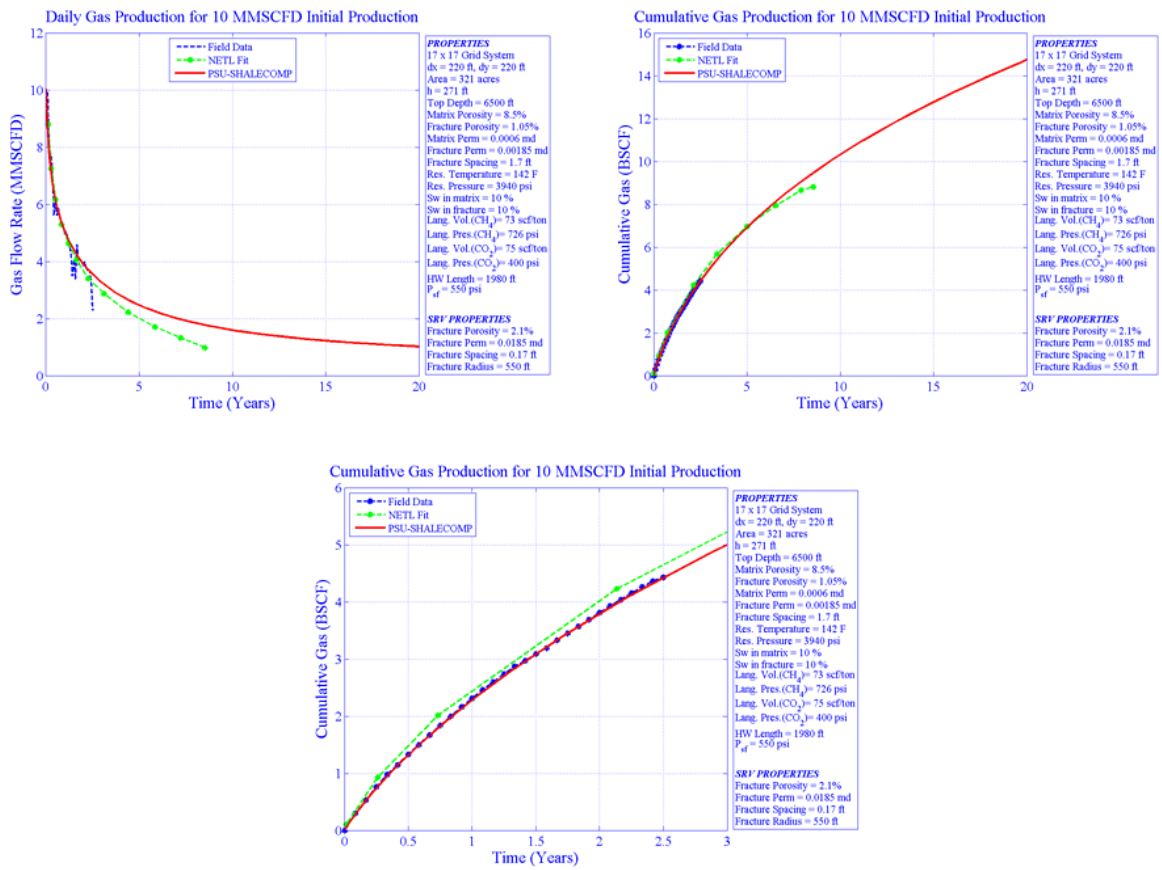

Figure 22: Mid-rate case history match.

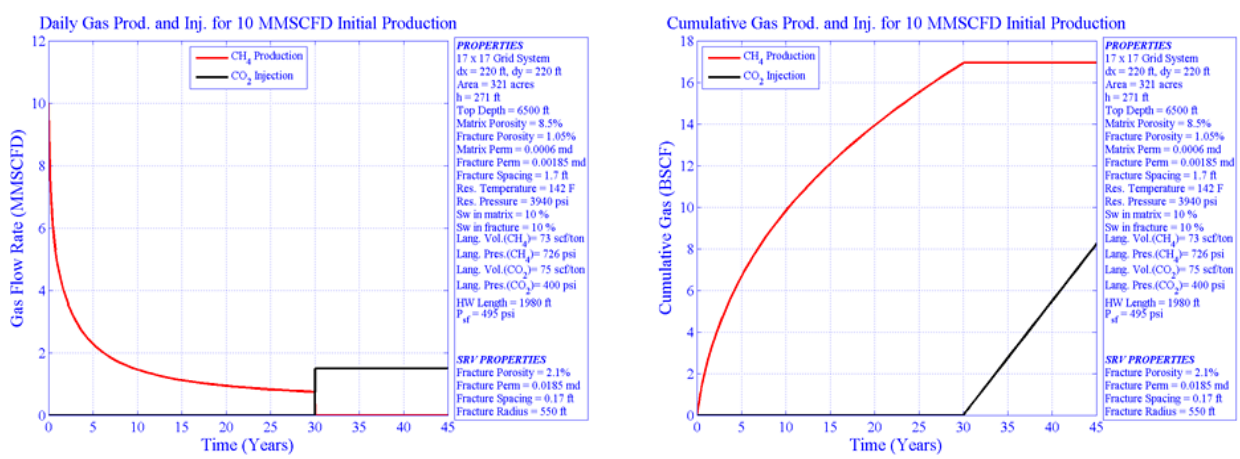

Figure 23: Mid-rate case pressure distribution.

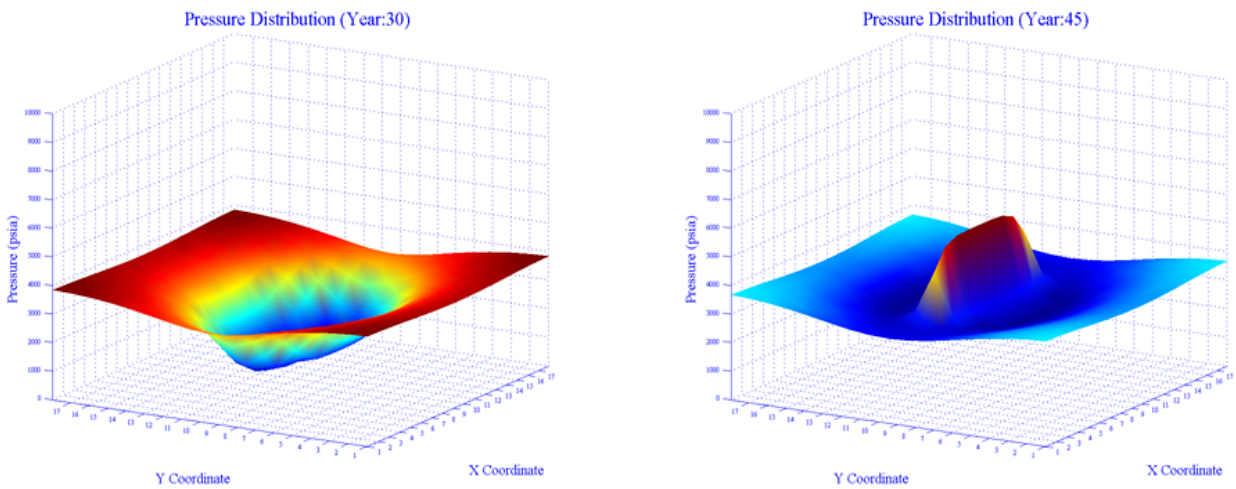

Figure 24: Mid-rate case production and injection performance.

The bottomhole pressure was set to 495 psi to match the initial production rate of 10 MMSCFD. The drainage area was depleted for a period of 30 years under these conditions. The average pressure of the drainage area at the end of 30 years of production was 2,970 psi. The average pressure of the SRV zone was 1,170 psi, and the average pressure of the unstimulated zone was 3,250 psi, with the average pressure of the well blocks at 980 psi. Such pressure distribution indicates that the reservoir can be depleted further, since the well is still capable of producing about 1 MMSCFD at the end of the 30th year. From these numbers one can conclude that:

- The average reservoir pressure is still high; the reservoir can be depleted further with the help of infill wells
- The average pressure in the SRV zone is rather close to the bottomhole pressure. Therefore, most of the CH_4 comes from the SRV zone
- The average pressure of the unstimulated reservoir is about 700 psi smaller than the initial reservoir pressure after 30 years of production. This observation again suggests that most of the production originates from the SRV zone
- Most of the injected CO_2 will only be stored in the SRV zone since the average pressure of the unstimulated reservoir is still in the neighborhood of the initial reservoir pressure. Also, formation fracturing pressure, which should not be exceeded throughout the injection period (formation fracture pressure is assumed as 5,000 psi in these simulations) constrains the volume of CO_2 injected

At the 30th year, the producer was altered to an injector to inject CO_2 at 1.5 MMSCFD. The simulation was stopped when the bottomhole pressure reached 5,000 psi. At this point in time (about 15th year of injection): the average pressure of the drainage area was about 3,210 psi; the average pressure of the SRV was 3,650 psi; the average pressure of unstimulated zone was 3,195 psi; and the average pressure of the well blocks was 4,900 psi. Again from these pressure values one can conclude that:

- The average pressure of the unstimulated reservoir is 50 psi smaller than the 30th year of depletion period. This indicates that either a very small amount of CO_2 or no CO_2 flows

through the unstimulated parts of the reservoir after 15 year of injection since the permeability is in the nanodarcy range

- The average pressure of the SRV zone is 3,650 psi, which is rather close to the initial reservoir pressure. Therefore, hydraulically fractured horizontal wells in shale formations are good candidates to sequester CO_2 since their ultra-tight characteristics make them a good source to store CO_2 in the long term

2.3 HIGH-RATE CASE INITIAL PRODUCTION

The reservoir area for this history match was determined to be 484 acres. The HWL and hydraulic fracture dimensions were adjusted to match the proposed initial production rate of 20 MMSCFD. Figure 25 indicates the daily flow rate and the cumulative production of CH_4 over the simulation period. It can be seen that PSU-SHALECOMP's results had a near-perfect match against the normalized field data using the SRV concept.

This model is rather large in terms of area. It can be seen that the well will produce nearly 2 MMSCFD at the end of the 30th year, making it highly economical. The cumulative production chart indicates that there are 32 BSCF of total CH_4 production and 27 BSCF of total CO_2 injection during this case simulation. The simulation was stopped at the end of the 51st year as the pressure constraint was reached.

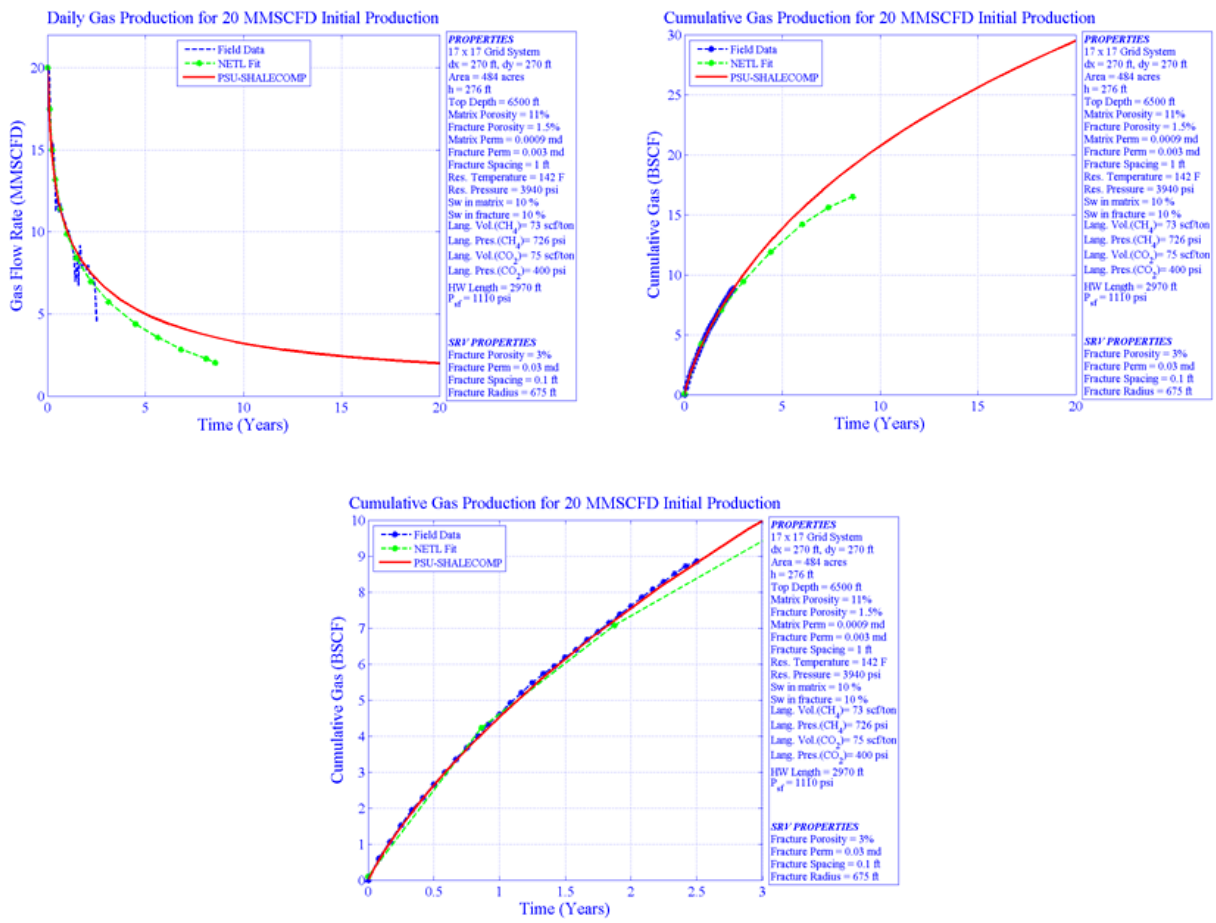

Figure 25: High-rate case history match.

CO_2 injection possibilities were investigated for the high-rate case (Figure 26). Since in this case the reservoir is almost 10 times larger than the low-rate case, injection well block pressures reach high pressures over a much longer time period. Also, the SRV zone is larger to meet the initial production criteria, which is 20 MMSCFD. This also aids in injecting larger volumes of CO_2.

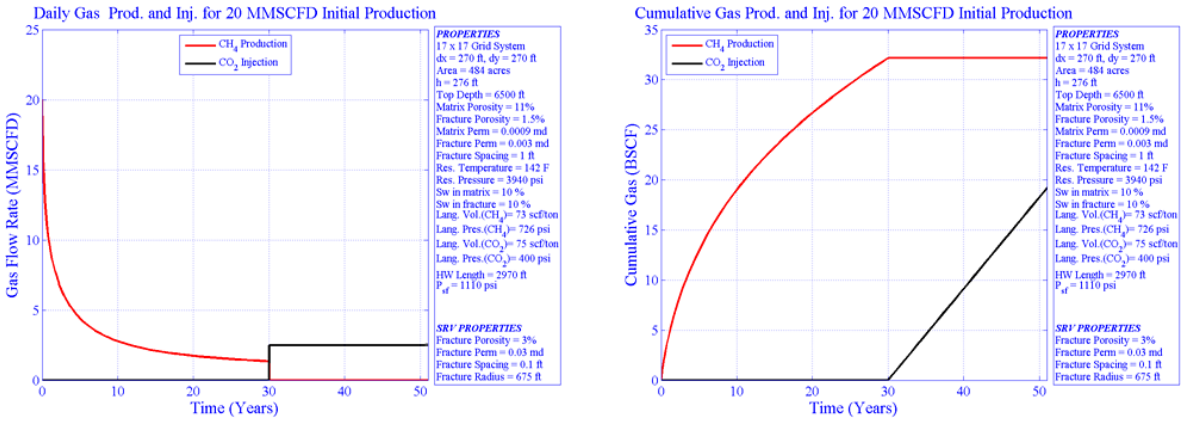

Figure 26: High-rate case production and injection performance.

2.4 CONCLUSIONS

Without hydraulic fracturing, volumetric flow rate of CO_2 in the unstimulated zone is quite small. The mole fraction of CO_2 in a neighboring unstimulated grid-block to a stimulated grid-block is only 5% after 30 years of injection (Figure 27).

From these case studies it can be concluded that to provide a good history match for the low-rate case (1 MMSCFD initial production rate), the lowest values need to be selected for thickness, fracture and matrix porosities, and fracture and matrix permeabilities from the ranges that are given in the DBD document, while the highest value must be selected for fracture spacing. Drainage area, HWL, and the SRV values should also be kept small as compared to mid-rate and high-rate cases.

Although the PSU-SHALECOMP simulator matched the normalized field data effectively, the low-rate case should not be considered as a practical scenario for production of CH_4 and injection of CO_2 because the drainage area (53 acres), horizontal wellbore length (500 ft), and SRV values were required to be unrealistically small. Accordingly, mid-rate and high-rate cases are considered to be more realistic scenarios for shale reservoirs. Accordingly, mid-rate and high-rate cases were used in most of the ongoing investigations.

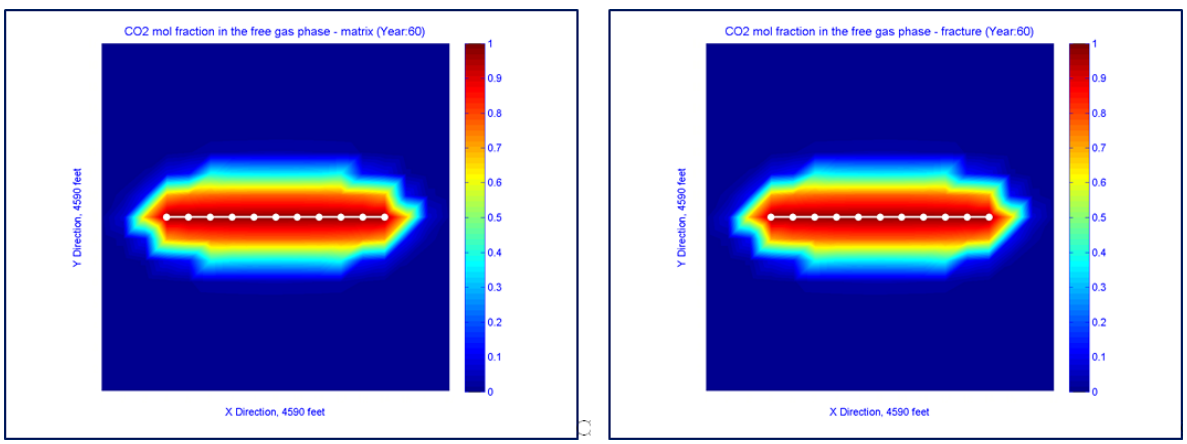

Figure 27: Mole fraction of CO_2 in the matrix and the fracture.

3. VARYING THE CO_2 INJECTION RATE AND LANGMUIR PRESSURES/VOLUMES

An investigation of eight different CO_2 injection rates was performed using PSU-SHALECOMP. The injection rates for the model were designed between 0.5 MMSCFD to 4 MMSCFD (Figure 28). These runs have a bottomhole pressure (BHP) constraint of 7,000 psi. The number of grid blocks in the model was increased from 17 to 25 to improve computational accuracy in the results.

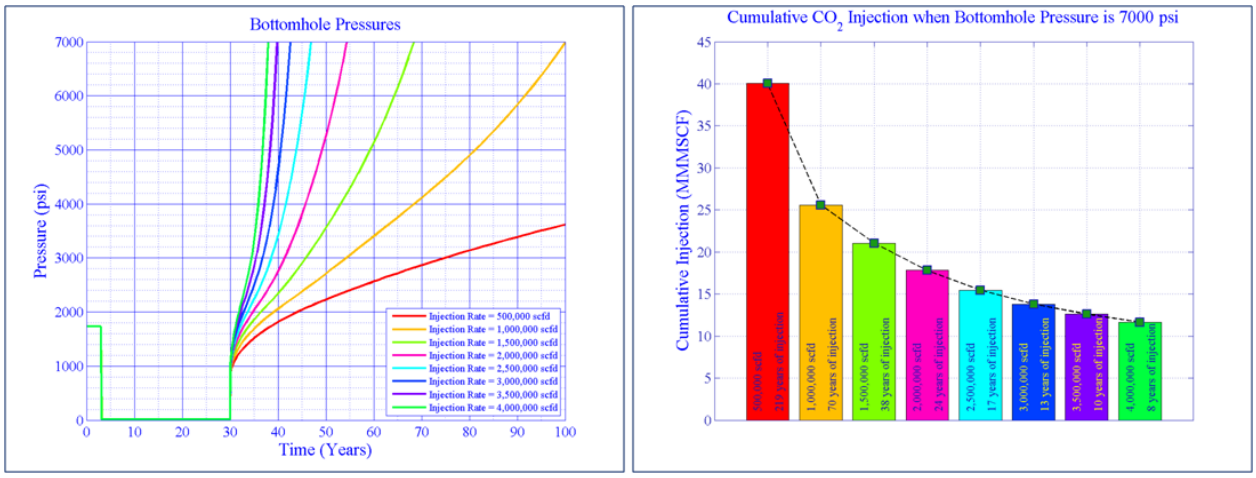

Figure 28: Production performances using varied CO_2 injection rates.

As expected, injection operations with higher injection rates result in larger and more rapid pressure increases in the block hosting the well and also at the injection face of the shale formation.

When implementing high injection rates, if the injected CO_2 is not given enough residence time while flowing through the sections of the SRV zone and also through the unstimulated reservoir sections, it will not be adsorbed effectively by the shale matrix depending upon the level of the limiting bottomhole pressure imposed at the injection well.

Lower injection rates can be more economical because of higher cumulative injection values and lower pumping costs. High injection rates also may cause initiation of undesired fractures and propagation through neighboring formations.

Cyclic repressurization of a depleted shale gas reservoir by CO_2 injection can help to increase the efficacy of the industrial CO_2 sequestration. Along the same lines, infill production/injection well drilling at locations which are not influenced by the injection operation is another option in converting a depleted shale gas reservoir to a CO_2 storage reservoir.

Parallel to investigations described above, additional runs were conducted for Dr. Seth Blumsack's team (PSU) to determine an optimum case for 30 years of continuous industrial CO_2 injection into a depleted shale gas reservoir. Initially, results for 1.5, 2, and 2.5 MMSCFD of constant CO_2 injection rates were provided. In the subsequent phase of these studies, a series of runs using 1.55, 1.6, and 1.65 MMSCFD of constant CO_2 injection into the same reservoir was

utilized. It is observed that the simulation run with 1.65 MMSCFD of constant CO_2 injection is the optimum case for 30 years of continuous industrial CO_2 injection for an 8,000 psi wellhead pressure constraint.

3.1 VARYING THE CO_2 INJECTION RATE FOR THE MID-RATE CASE

An investigation of 10 different injection rates for the mid-rate case was carried out using PSU-SHALECOMP (Table 2). All of the injection rates were taken from industrial CO_2 sources such as steel, paper, and coal plants. This data was provided by Dr. Blumsack's team at PSU. The runs had a BHP constraint of 7,000 psi. Most of the models do not reach 7,000 psi in a given injection time of 30 years. The number of grid blocks in the model was increased from 17 to 25 to improve computational accuracy in the results.

As anticipated, injection operations with higher injection rates result in larger and more rapid pressure increases in the blocks hosting the well and also at the injection face of the shale formation.

Table 2: Mid-rate Case Injection Rates

CO_2 Injection Rate (MMSCFD)	$P_{bhp\text{-}final}$ (Final Bottomhole Pressures, psi)	Years of Injection
1.437	4,843	30
1.330	4,388	30
1.093	3,636	30
1.663	6,205	30
1.606	5,790	30
0.722	2,872	30
2.660	> 7,000	15
2.186	> 7,000	21
4.990	> 7,000	6
1.310	4,313	30

3.2 MODEL INTEGRATION OF WEATHERFORD LANGMUIR PRESSURES AND VOLUMES

An investigation was initiated using the new Langmuir pressures and Langmuir volumes, which were provided by Weatherford. Langmuir pressures and volumes for five different samples were investigated by maintaining the reservoir and wellbore parameters. Total volumes of injected CO_2 values were compared (Table 3). Also, total adsorbed amounts of CO_2 were examined. It was observed that adsorption vs. free gas ratios can range up to 20%, which is higher than what has been typically observed in previous studies. Some of the experimental data for Langmuir pressures and volumes are considered large as they were obtained from powdered samples of Marcellus shale.

Table 3: Weatherford Sorption Isotherm Data

	CH_4		CO_2	
Sample	**Adsorption rate (SCF/ton)**	**Adsorption Pressure (psi)**	**Adsorption rate (SCF/ton)**	**Adsorption Pressure (psi)**
F1	37.23	3,426.14	89.22	897.67
F2	22.88	4,252.19	84.23	2,748.78
F3	32.37	1,344.01	135.83	1,346.22
F4	113.96	7,436.49	163.87	1,350.30
F5	20.37	3,088.98	61.65	582.52

Figure 29 below shows the total CO_2 injected when the BHP reaches 4,500 psi and the ratios of CO_2 in the adsorbed and free gas phases for each of the cases. The chart on the left indicates that samples F4, F3, and F1 had slightly higher cumulative injection of CO_2.

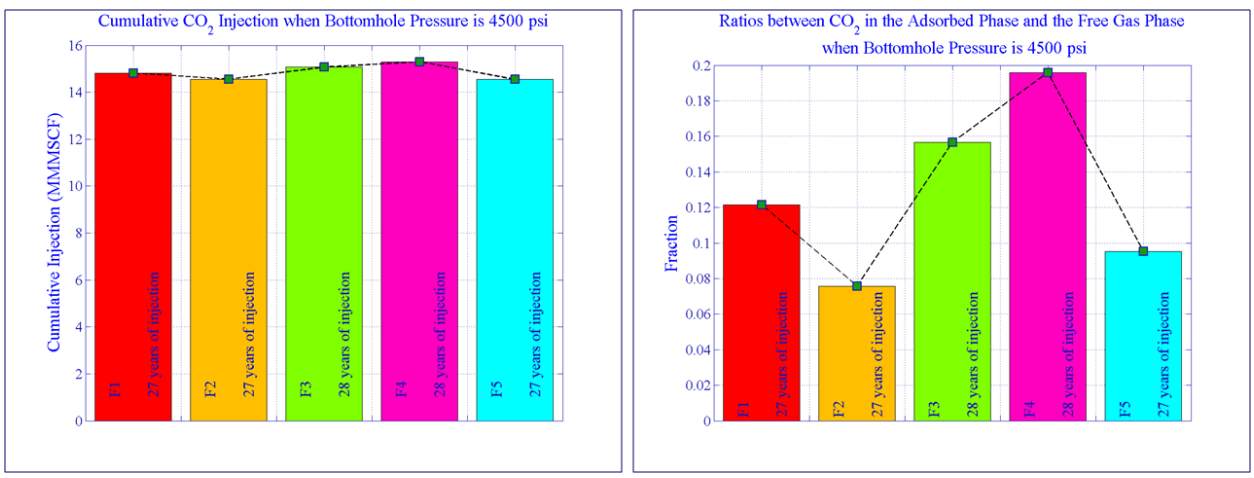

Figure 29: Cumulative production values and desorption fractions for mid-rate case at 4,500 psi.

The chart on the right shows the adsorbed phase vs. free gas phase ratios. It can be seen that F4 can adsorb almost 20% of the total injected gas at 4,500 psi. F4 would be a better CO_2 sequestration candidate than F2 or F5. The simulated injection performance for the mid-rate case using these five samples is summarized in Table 4.

Table 4: Simulated Mid-rate Case Injection Performance for Five Samples at 4,500 psi BHP

Sample	Cumulative CO_2 Injected (BSCF)	Cumulative CO_2 Adsorbed (BSCF)	Cumulative CO_2 Free Gas Phase (BSCF)	Cum. CO_2 Adsorbed/Cum. CO_2 Free Gas Phase	Days of Injection
F1	14.8	1.61	13.2	0.122	9,874
F2	14.6	1.02	13.5	0.076	9,704
F3	15.1	2.14	13.7	0.157	10,046
F4	15.3	2.51	12.8	0.196	10,199
F5	14.5	1.28	13.5	0.095	9,837

4. PARAMETRIC STUDY OF FOUR PROJECT DESIGN PARAMETERS

An investigation involving four different project design parameters for the mid-rate case including: horizontal wellbore length; SRV fracture permeabilities; SRV fracture porosities; and SRV fracture spacing was carried out using PSU-SHALECOMP with the following observations.

4.1 HORIZONTAL WELLBORE LENGTH

The first parameter was the investigation of different HWLs for the mid-rate case. In this case, six different HWLs were examined. All of the other input parameters remained the same including CO_2 injection rate, which is fixed at 1.5 MMSCFD. HWL plays an important role on production and injection performances (Table 5).

Table 5: Cumulative Injected and Adsorbed CO_2 Volumes Achieved with Different HWLs

Horizontal Wellbore Length (ft)	Cumulative CO_2 Injected (BSCF)	Cumulative CO_2 Adsorbed (BSCF)	Cumulative CO_2 Free Gas Phase (BSCF)	Cum. CO_2 Adsorbed/Cum. CO_2 Free Gas Phase
1,235	4.62	0.581	4.04	0.144
1,588	7.33	0.864	6.46	0.134
1,941	10.6	1.18	9.44	0.125
2,294	14.4	1.50	12.9	0.116
2,647	18.4	1.81	16.6	0.109
3,000	22.5	2.05	20.5	0.100

Shorter wellbore lengths reach BHP restriction in a much shorter period of time. The CO_2 injection rates are increased in longer wellbores enabling the injection of CO_2 more effectively as the reservoir contact area increases. Figure 30 shows the total CO_2 injected when the BHP reaches 7,000 psi and the ratios of CO_2 in the adsorbed and free gas phases for each of the cases as HWL is increased.

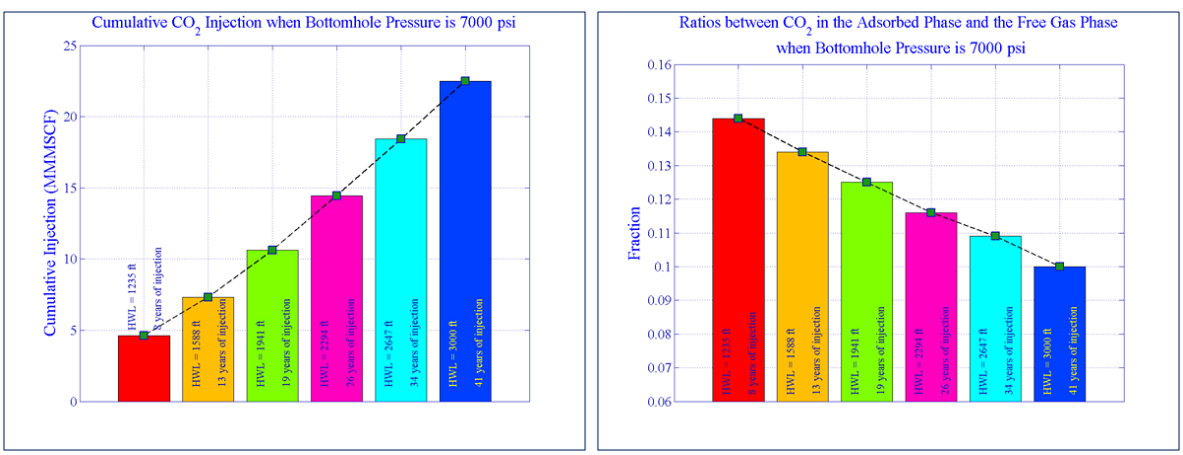

Figure 30: Effect of varying HWL on production when using the mid-rate case.

4.2 SRV FRACTURE PERMEABILITY

Different SRV fracture permeability values were investigated for the mid-rate case. Five different SRV fracture permeability values (0.00185, 0.00925, 0.0185, 0.02775, and 0.037 md) were used in this investigation. SRV fracture permeabilities were increased by multiples of 1, 5, 10, 15, and 20 of the natural fracture permeability values. It was observed that it is essential to obtain higher fracture permeabilities within the SRV zone to be able to effectively produce CH_4 and inject CO_2. In Figure 31 the charts show the production/injection performances when comparing different SRV fracture permeability values. The displaced results indicate that fracture permeability has a major impact on production and injection performances.

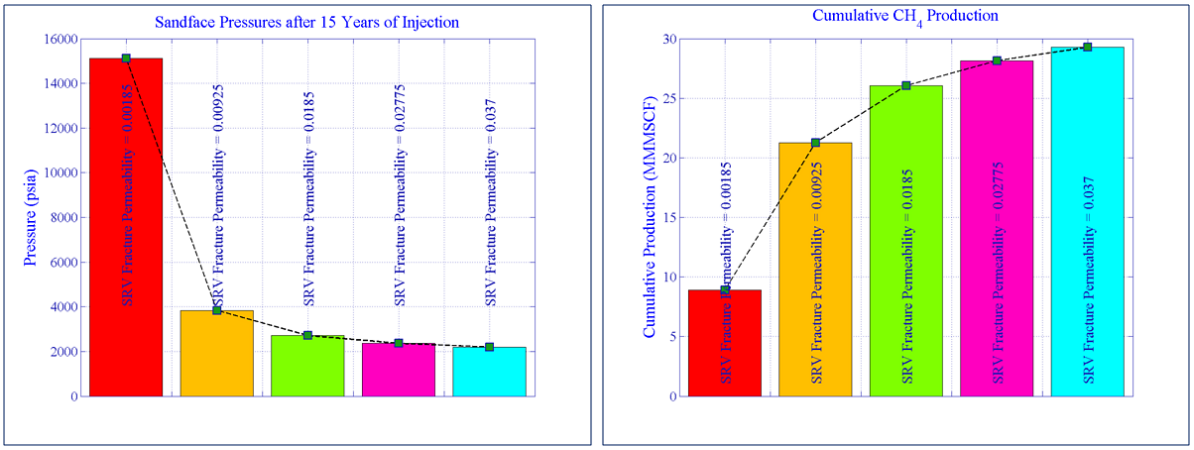

Figure 31: Effect of varying fracture permeability on production when using the mid-rate case.

4.3 SRV FRACTURE POROSITY

An investigation was conducted on the effect of different SRV fracture porosity values (0.012, 0.015, 0.018, 0.021, and 0.024) on production/injection performance. SRV fracture porosities are increased by multiples of 1.2, 1.5, 1.8, 2.1, and 2.4 of the natural reservoir fracture porosities. It was observed that SRV fracture porosity values have a pronounced effect on BHP, which may lead to longer injection times. The same mid-rate model was considered as the base model for this investigation. The CO_2 injection rate was set to 1.5 MMSCFD.

In Figure 32 the charts show the production/injection performances for different SRV fracture porosity values. It is clear that fracture porosity has a relatively small impact on cumulative production. The bar chart on the right shows the bottomhole injection pressure values encountered for different SRV fracture porosity values. Larger SRV fracture porosity values have lower bottomhole pressure values, which in turn, increases the duration of the CO_2 injection period.

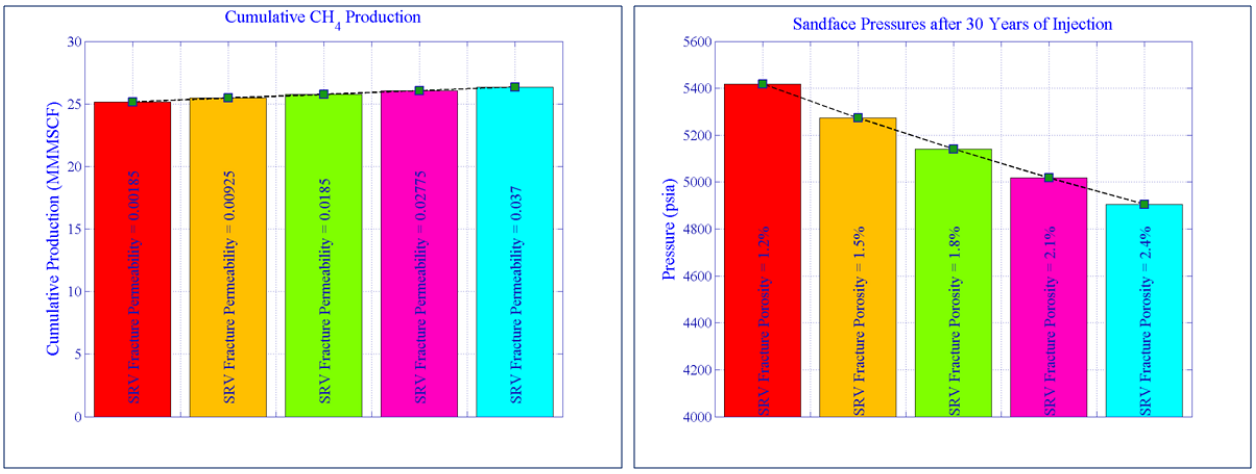

Figure 32: Effect of varying fracture porosity on production when using the mid-rate case.

4.4 SRV FRACTURE SPACING

The effect of varying SRV fracture spacing values was investigated for the mid-rate case. Six different SRV fracture spacing scenarios were considered (0.131, 0.170, 0.243, 0.850, and 1.7 ft).

In Figure 33 the charts show the effect of SRV fracture spacing values on the production and injection performances. As the fracture spacing value becomes smaller the storage capacity of the matrix becomes smaller. This is reflected with an increase in BHP at the smaller end of the fracture spacing.

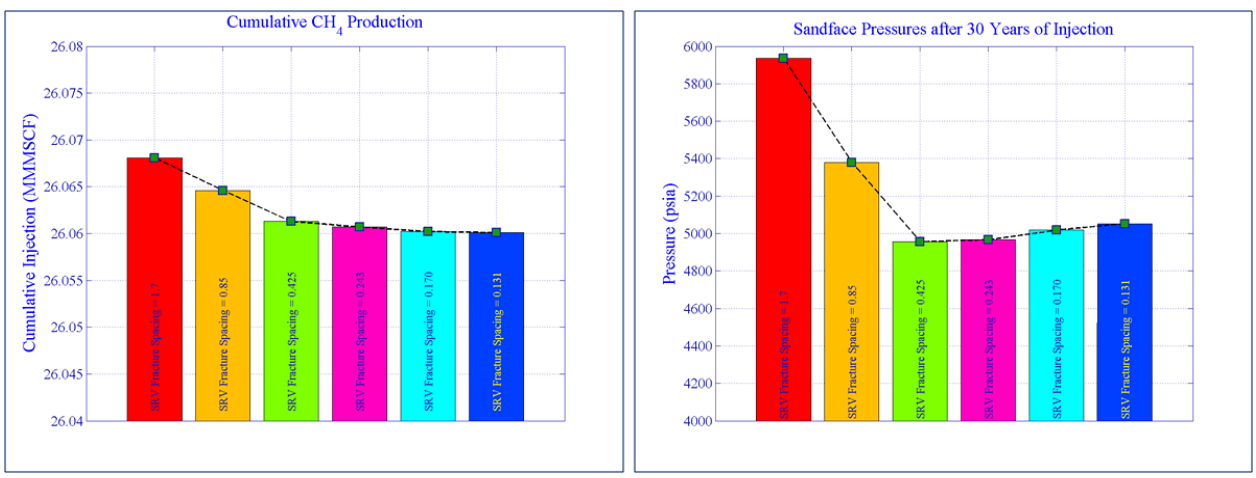

Figure 33: Effect of varying fracture porosity on production when using the mid-rate case.

5. THE EFFECT OF ALLOWING PERMEABILITY MODIFICATION AS A FUNCTION OF PORE PRESSURE WITHIN THE PSU-SHALECOMP MODEL

Absolute matrix permeability values were modified using the given experimental data (Figure 34) provided by Dr. Aminian's team at WVU. The convergence rate of the simulator was adversely affected when the permeability values were updated at the end of each model iteration. In order to speed up the run times, the number of grid blocks was decreased in the simulation and the results obtained indicate that within the ranges of the experimental data on permeability changes, no significant differences in injection and production performances were encountered. At this stage, this observation is attributed to the dominance of Fickian flow (diffusion) when compared to Darcian flow (laminar) within the range of matrix permeabilities studied.

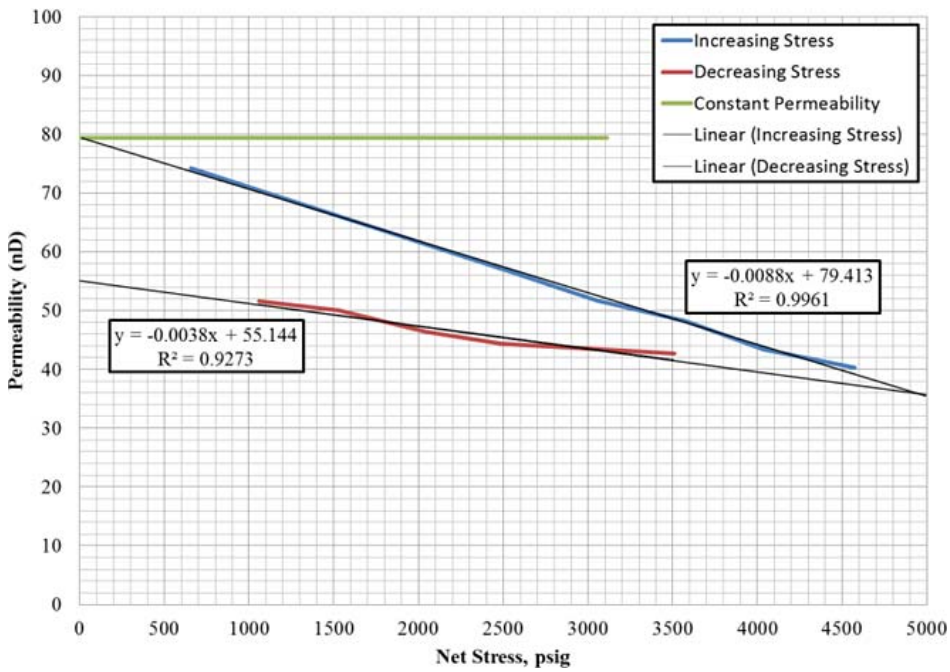

Figure 34: Effect of net stress on average permeability.

An investigation on the effect of permeability modification within the PSU-SHALECOMP model was conducted according to the experimental data provided in the DBD (Table 3-3, see Appendix A). Two different scenarios were investigated. In the first scenario, the matrix and fracture permeabilities were kept close to Marcellus shale average permeability values, which are 0.0006 md for the matrix and 0.00185 md for the natural fractures. In the second scenario, the matrix and fracture permeabilities were increased by three orders of magnitude to make the effect of change in permeabilities more pronounced as the changes in net stress values become much greater.

The simulation studies were performed using coarse grid block systems as it was decided to implement the same experimental data on modification of both matrix and fracture permeabilities. Previously, only matrix permeability modifications were investigated.

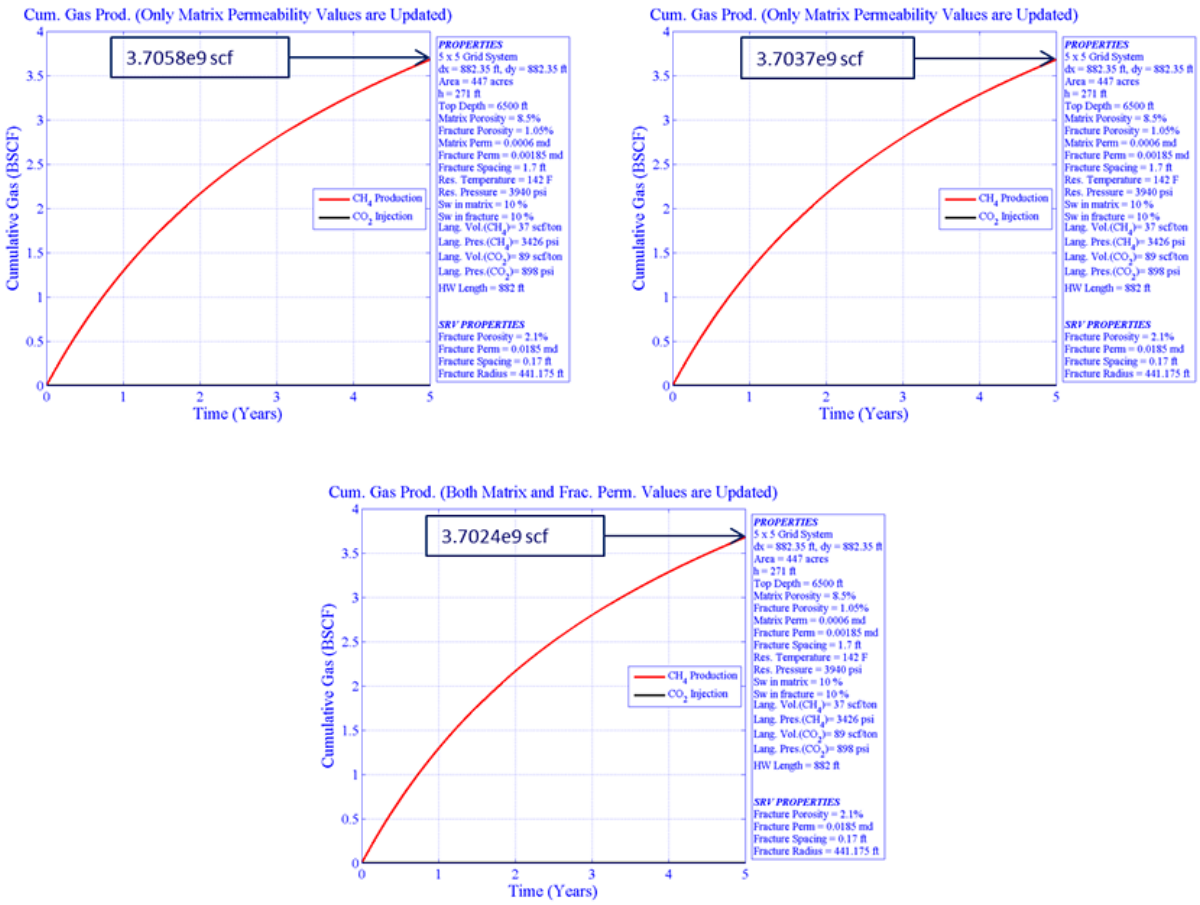

Figure 35: Effect of permeability modification on production performance.

The results obtained (Figure 35) indicate that within the ranges of the experimental data on matrix and fracture permeability changes, no substantial changes in injection and production performances were encountered both in the low and high permeability cases because the changes in permeability values are negligibly small so that no significant impact of permeability changes on production or injection performance were observed.

The chart on the top-left shows cumulative production of the unchanged permeability case. In this case, the total production is 3.7058 BSCF after five years.

The chart on the top-right shows the cumulative production of the second case. In this case only matrix permeability values of the formation were modified. The cumulative production is 3.7037 BSCF after 5 years. The difference between these two cases over a 5-year period is about 2.1 MMSCF, which is a negligibly small volume.

The chart on the bottom is the third case where both matrix and fracture permeabilities were modified. The difference between the first case and this case at the end of the fifth year of production is about 3.4 MMSCF (a volume equivalent to one day of production during the sixth month of any of the cases).

It is expected that changes in absolute permeability values as a function of changes in pore pressure values will have an effect both in the CH_4 production and subsequent CO_2 injection

cycles of the modeling studies. During the production cycle as the production of CH_4 continues the net stress on the system will increase and the permeability of the medium will decrease. It is expected that the total CH_4 production will be less at the end of a production period of 30 years and also the average reservoir pressure will be at a higher level as compared to what is currently observed when changes in the permeability values are ignored.

During the injection of CO_2, pore pressure will continuously increase causing a decrease in net stress which will result in an increase in absolute permeability of the system, permitting injection of more CO_2 at the time when the imposed pressure constraint at the injection point is encountered. However, it should not be forgotten that at the time the injection is started the reservoir is at a higher average pressure; therefore, the window of opportunity in terms of permissible incremental pressure increase during the injection period can be shorter.

6. MONTE CARLO SIMULATION STUDIES AND OTHER SENSITIVITY ANALYSES

6.1 INITIAL MONTE CARLO SIMULATION STUDY

An initial Monte Carlo simulation study was conducted with a total of 1,000 model runs conducted for randomly generated thickness, matrix porosity, fracture porosity, matrix permeability, fracture permeability, and fracture spacing values. In all of the runs, the shale reservoir was depleted for 30 years, then it was followed by another 30 years of CO_2 injection.

The results of Monte Carlo simulation study indicate that the uncertainty for original gas in place (OGIP) is quite large, varying between 95 BSCF to 175 BSCF. However, the cumulative CH_4 production frequency figure has a triangular distribution where the highest probability for 30 years of CH_4 production is found to be in the range of 22 BSCF to 26 BSCF over a drainage area of 492 acres.

Monte Carlo analysis also indicated that there is a 90% probability that 15.3 BSCF of CO_2 can be injected into the reservoir over a 30-year period. This translates to an injection capacity of 31.1 MMSCF per acre over 30 years.

A history match exercise parallel to the National Energy Technology Laboratory (NETL) NFFLOW's history-match was conducted. In order to be able to obtain a good quality history match, fracture porosity and fracture permeability were selected from the ICMI DBD (Table 3-2, Appendix A). Also, the SRV porosity and SRV permeability values were increased and hydraulic fracture spacing in the SRV zone values were decreased to obtain the history match presented in this report.

6.2 DETAILED MONTE CARLO SIMULATIONS

Two Monte Carlo simulation studies were conducted as a total of 1,500 model runs were made for randomly generated thickness, matrix porosity, fracture porosity, matrix permeability, fracture permeability, fracture spacing, Langmuir volume constants for CH_4 and CO_2, and Langmuir pressure constants for CH_4 and CO_2. In all of the realizations, the well was put on production for 30 years and followed by another 30 years of CO_2 injection. In the first Monte Carlo simulation, a specified injection pressure of 5,000 psi was utilized (Figure 36 and Figure 37). The second Monte Carlo simulation study was conducted for a specified injection rate of 1.5 MMSCFD (Figure 38 and Figure 39).

The results of Monte Carlo simulation study indicate that the uncertainty for OGIP is quite large, varying between 95 BSCF to 180 BSCF over the total acreage of 493 acres. However, the cumulative CH_4 production frequency figure has a triangular distribution indicating that the highest probability for 30 years of CH_4 production is in the range of 16 BSCF to 30 BSCF.

Monte Carlo analysis also indicated that there is a 90% probability (P_{90}) that 15.3 BSCF of CO_2 can be injected over a period of 30 years.

In the second Monte Carlo simulation study, the P_{90} value is determined to be 20.1 BSCF for 30 years of CH_4 production. Similarly, the P_{90} value is determined to be 11.6 BSCF for 30 years of CO_2 injection.

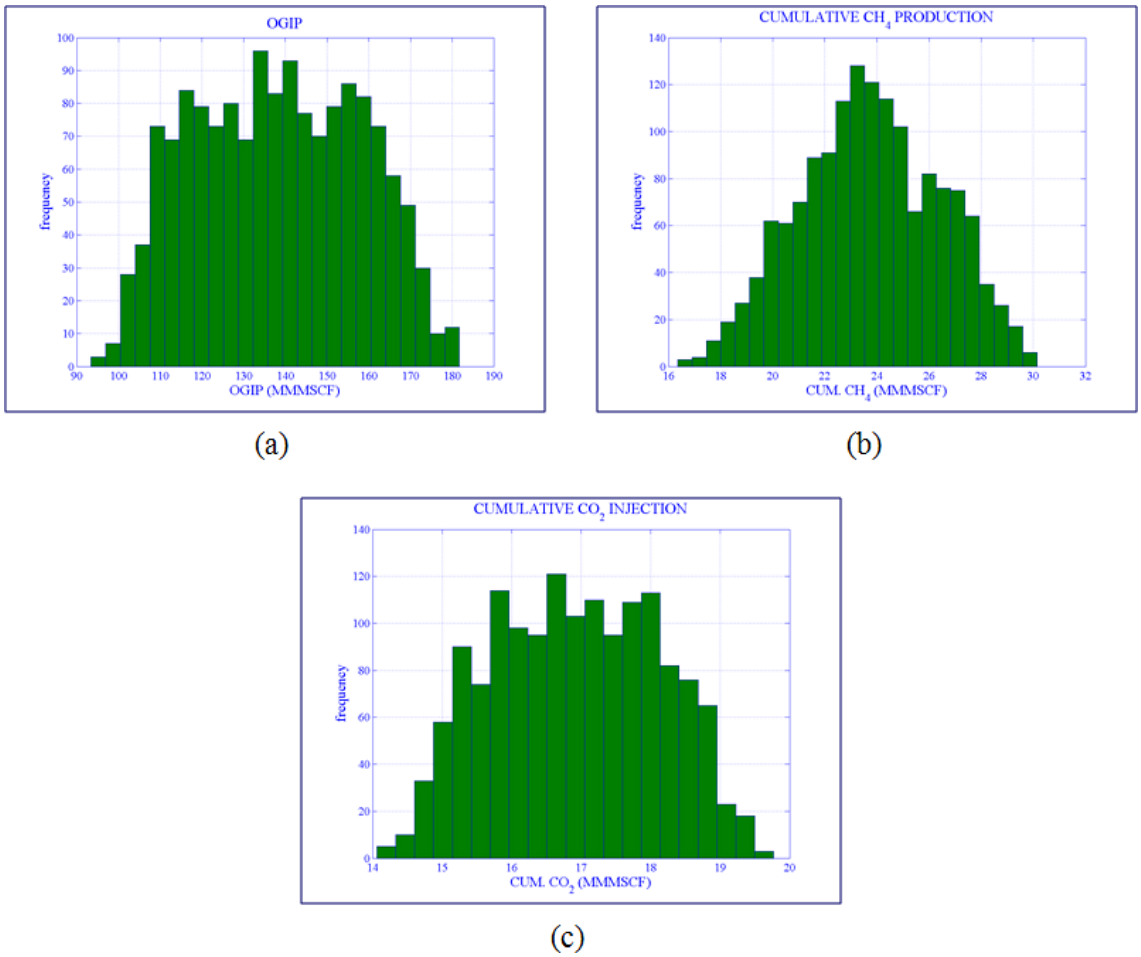

Figure 36: Detailed Monte Carlo simulation at constant pressure (5,000 psi) - 1 frequency function: (a) OGIP, (b) cumulative CH_4 production, and (c) cumulative CO_2 injection.

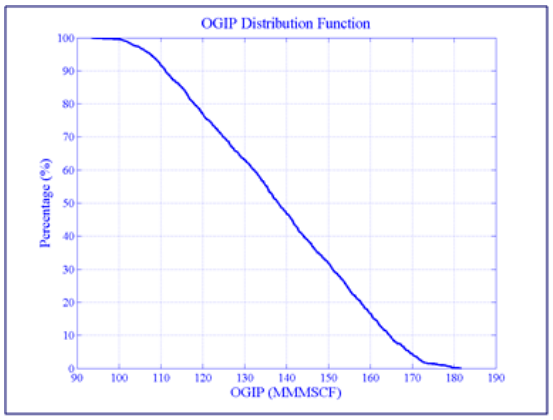

(a)

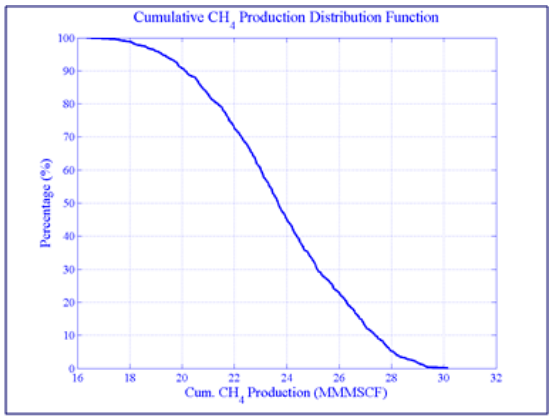

(b)

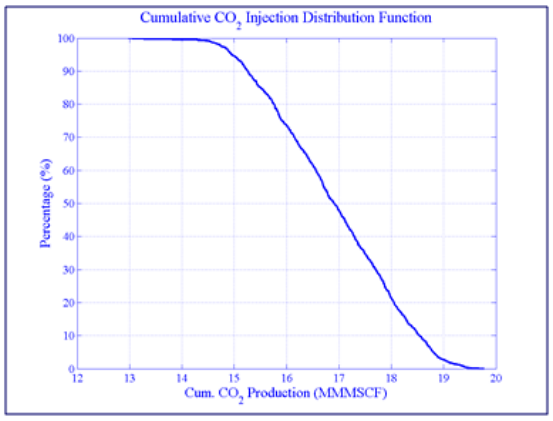

(c)

Figure 37: Detailed Monte Carlo simulation at constant pressure (5,000 psi) - 1 frequency function: (a) OGIP, (b) cumulative CH_4 production, and (c) cumulative CO_2 injection.

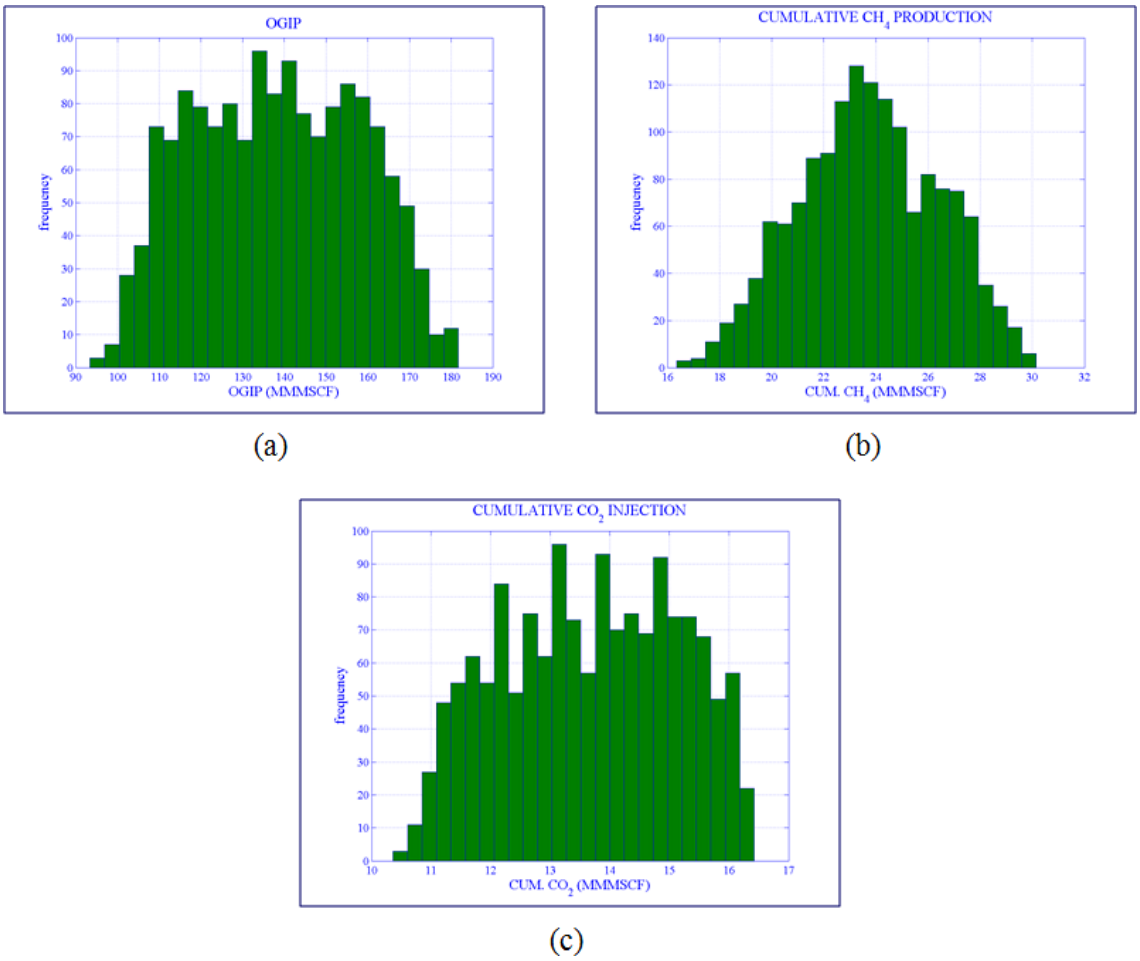

Figure 38: Detailed Monte Carlo simulation at constant injection rate (1.5 MMSCFD) - 1 frequency function: (a) OGIP, (b) cumulative CH_4 production, and (c) cumulative CO_2 injection.

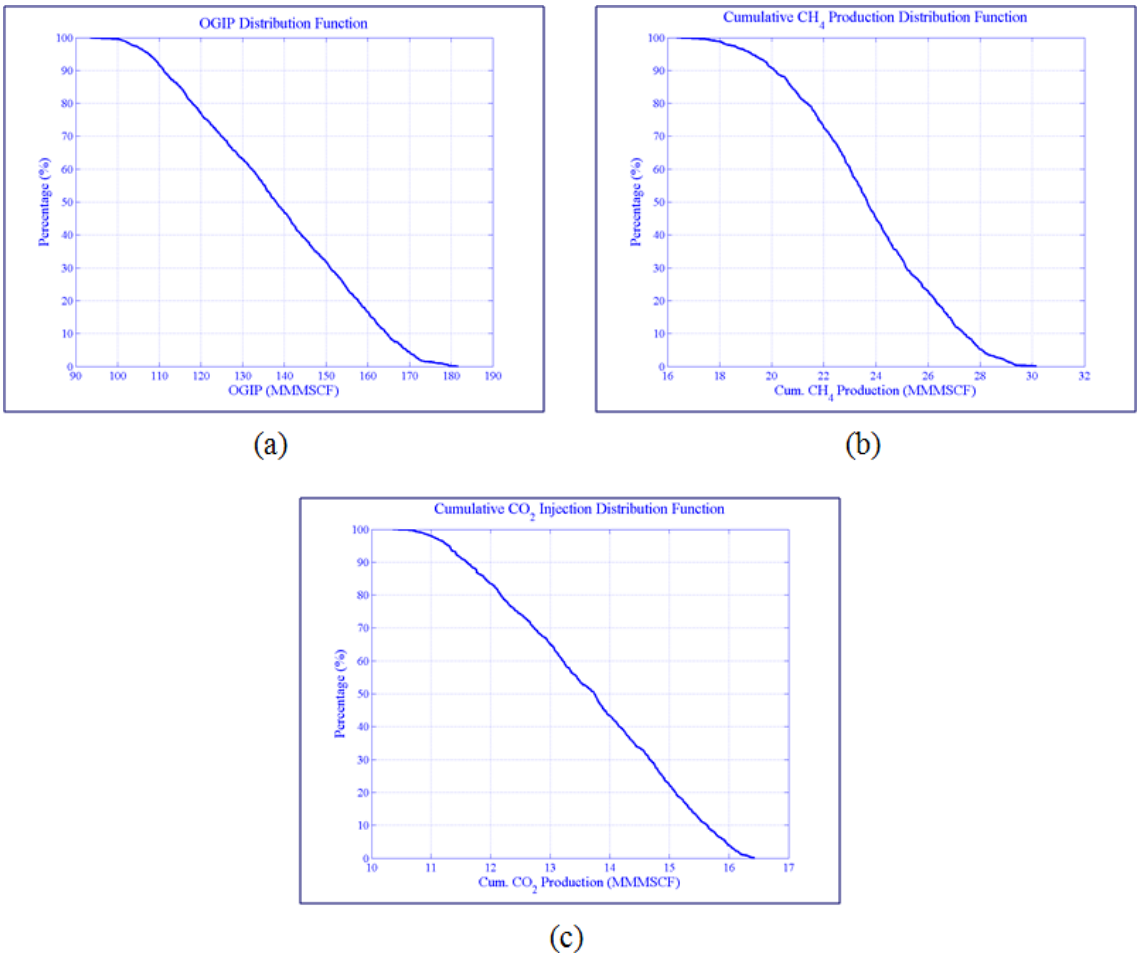

Figure 39: Detailed Monte Carlo simulation at constant injection rate (1.5 MMSCFD) - 1 distribution function: (a) OGIP, (b) cumulative CH_4 production, and (c) cumulative CO_2 injection.

6.3 GRID SIZE SENSITIVITY

A total of 30 different models' results were analyzed for different numbers of grid blocks that vary from 17 × 17 to 27 × 27. This was a demanding study as horizontal wellbore lengths, SRVs and reservoir drainage areas are needed to be identical for all of the model runs. Similar production profiles were generated for all of the models considered. Coarse models have shorter simulation times. However, pressure profiles, molar concentration distributions of the components, etc., are as not as accurate as fine models, as shown in the two charts at the bottom of Figure 40.

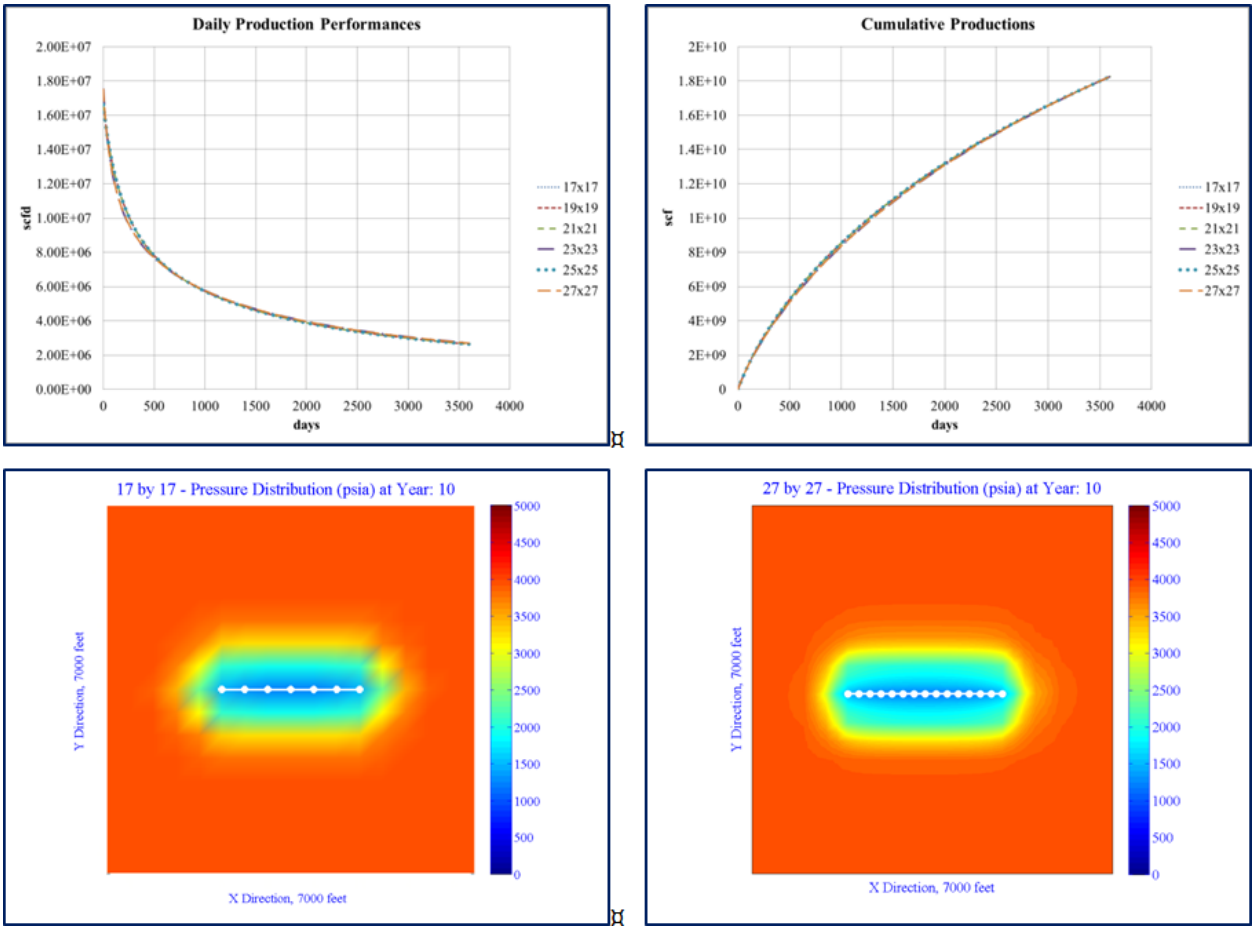

Figure 40: Illustration of model sensitivity to varying grid block size on a) lateral gas production profile, and b) formation pressure distribution.

6.4 PRODUCTION/INJECTION PERFORMANCE FOR DIFFERENT HWLS AND WING SIZE

Production performances of different HWLs were investigated for a range between 1,000 and 3,500 ft. The other reservoir parameters were unchanged. The model was developed from Monte Carlo Simulations representing the mid-rate case. Two simulations were investigated for different hydraulic fracture half wing lengths, which are 600 ft and 800 ft. Results for this sensitivity analysis are summarized in Table 6 and 7.

Table 6: Production/Injection Effects from Varying HWLs with 600 ft Half-Wing Lengths

Horizontal Wellbore Length (ft)	Original Gas in Place (BSCF)	Cumulative CH_4 Production (BSCF)	Recovery Factor (30 years)	Cumulative CO_2 Injection (BSCF)	CO_2 Injection/CH_4 Production Ratio	Years of CO_2 Injection
1,250	270	15	0.056	4	0.267	5
1,500	270	18	0.065	5	0.278	7
1,750	270	20	0.074	6	0.300	9
2,000	270	23	0.083	8	0.348	11
2,250	270	25	0.091	9	0.360	13
2,500	270	27	0.100	11	0.407	15
2,750	270	30	0.109	12	0.400	17
3,000	270	32	0.117	14	0.438	19
3,250	270	34	0.125	16	0.471	22

Table 7: Production/Injection Effects from Varying HWLs with 800 ft Half-Wing Lengths

Horizontal Wellbore Length (ft)	Original Gas in Place (BSCF)	Cumulative CH_4 Production (BSCF)	Recovery Factor (30 years)	Cumulative CO_2 Injection (BSCF)	CO_2 Injection/CH_4 Production Ratio	Years of CO_2 Injection
1,000	270	14	0.050	3	0.249	4
1,250	270	16	0.061	5	0.283	6
1,500	270	19	0.071	6	0.315	8
1,750	270	22	0.081	8	0.344	10
2,000	270	25	0.091	9	0.370	12
2,250	270	27	0.101	11	0.394	15
2,500	270	30	0.110	12	0.417	17
2,750	270	32	0.120	14	0.439	19
3,000	270	35	0.129	16	0.457	22
3,250	270	37	0.138	18	0.478	24
3,500	270	40	0.147	20	0.497	27

All of the comparisons show a linear behavior with the increasing horizontal wellbore length and the rest of the reservoir parameters are unchanged. An economic analysis is required to determine the optimum scenario for both cumulative production and CO_2 injection cases.

6.5 PRODUCTION/INJECTION PERFORMANCE FOR DIFFERENT HYDRAULIC FRACTURE SPACING IN THE SRV ZONE

Table 8 summarizes the effects of different hydraulic fracture spacing in the SRV zone on production and injection performance. As the fracture spacing value becomes smaller, the injected CO_2 will be distributed more uniformly through the broken shale formation because there are more hydraulically created fractures in the system. As a result pressure levels in the SRV zone increase at a much slower pace. As previously mentioned the Langmuir volume constant for CO_2 is slightly higher than the one for that of CH_4. These two factors contribute to larger storage values achieved during CO_2 injection as compared to the produced volumes of CH_4.

Table 8: Production/Injection Effects from Varying Hydraulic Fracture Spacing

SRV Fracture Spacing (ft)	Original Gas in Place (BSCF)	Cumulative CH_4 Production (BSCF)	Recovery Factor (30 years)	Cumulative CO_2 Injection (BSCF)	CO_2 Inj/CH_4 Prod Ratio (x year of CO_2 Inj)	Injection Period (years)	Year CO_2 Injection Stops
1.70	121	26	0.21505	12.9	0.496	23.6	53.6
0.850	121	26	0.21502	13.9	0.532	25.3	55.3
0.425	121	26	0.21499	14.9	0.573	27.3	57.3
0.243	121	26	0.21512	14.9	0.572	27.2	57.2
0.170	121	26	0.21498	14.7	0.566	26.9	56.9
0.131	121	26	0.21498	14.6	0.561	26.7	56.7

7. HISTORY MATCHING OF FIELD DATA FOR A SINGLE-LATERAL PAD

7.1 DAILY AND CUMULATIVE GAS PRODUCTION

Four different simulations were run for history matching with the single-lateral pad. The first three of the simulations have the same reservoir and SRV parameters. However, different BHP values were tested to determine the production performance of the simulations.

In Simulation 1, BHP was set to 15 psi to evaluate the maximum capacity of the given reservoir (Figure 41). The initial production value was much higher (22 MMSCFD) than the normalized field data (which was set as 10 MMSCFD).

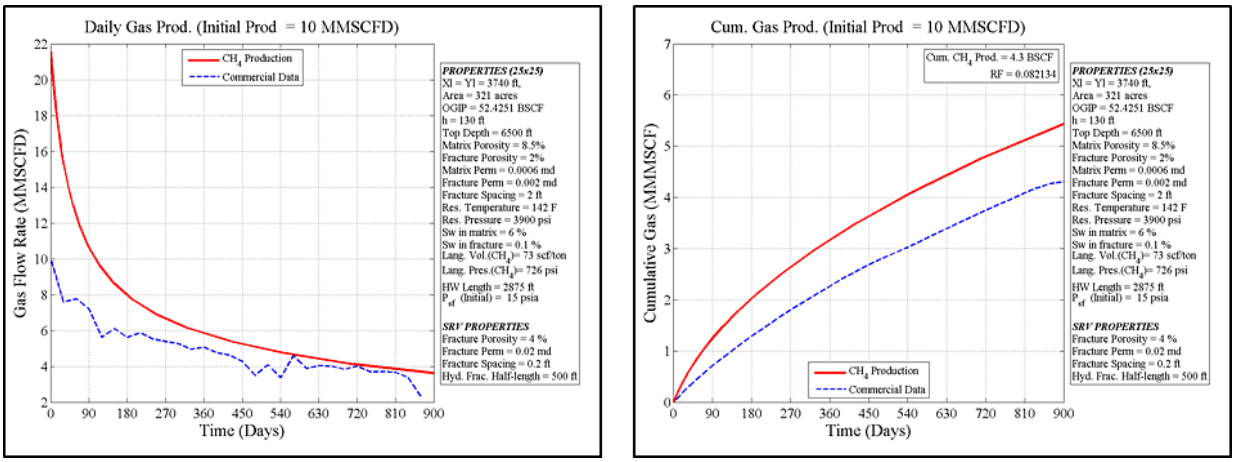

Figure 41: Single-lateral pad, Simulation 1 production performance.

In Simulation 2 (Figure 42), the initial production value was matched and the BHP was set to 2,100 psi. However, it was determined that this BHP value was rather high to deplete the drainage area efficiently.

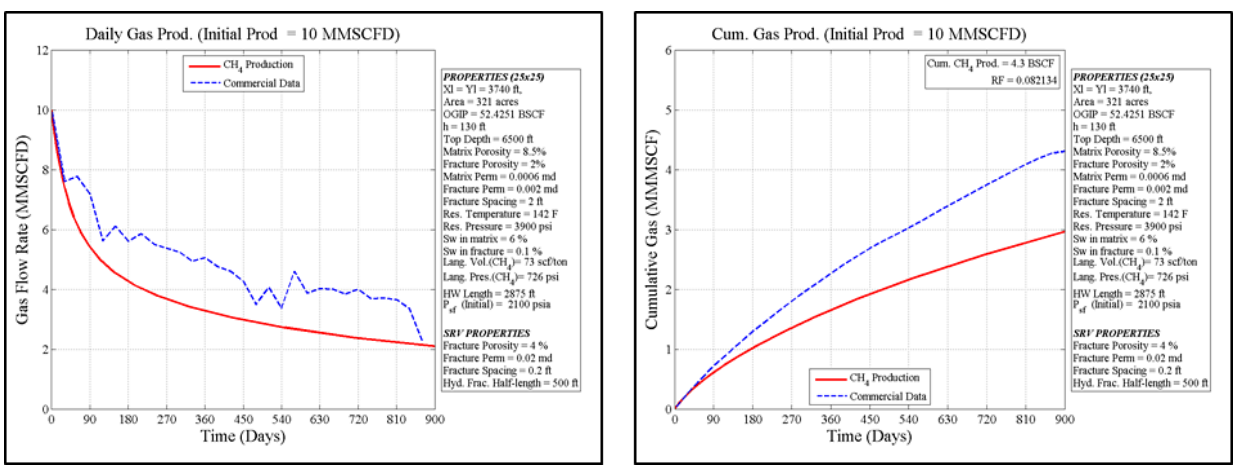

Figure 42: Single-lateral pad, Simulation 2 production performance.

Simulation 3 (Figure 43) has different BHP values for the first 30 months to generate a good history match by honoring the given field data. The history match that was obtained by altered BHP values matched the field data very closely. The BHP value at the 30th month was set to 15 psi to deplete the formation as much as possible.

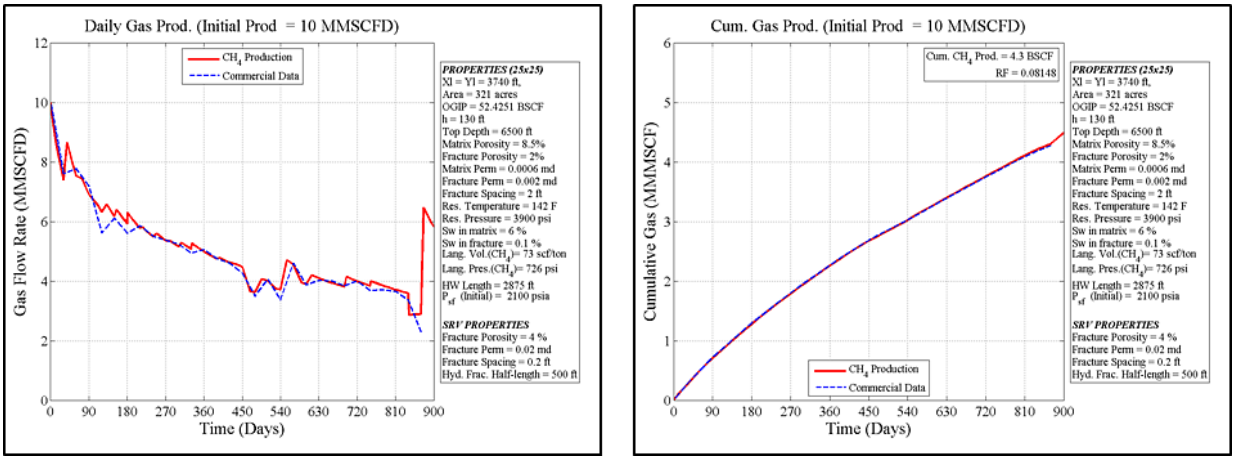

Figure 43: Single-lateral pad, Simulation 3 production performance.

Simulation 4 (Figure 44) utilized higher SRV fracture porosity (28%) to generate a good fit to the production field data. It was observed that SRV fracture porosity has a significant impact on behavior of the production performance in history matching studies. The assigned porosity value was not realistic, but it was used to test the response of the model.

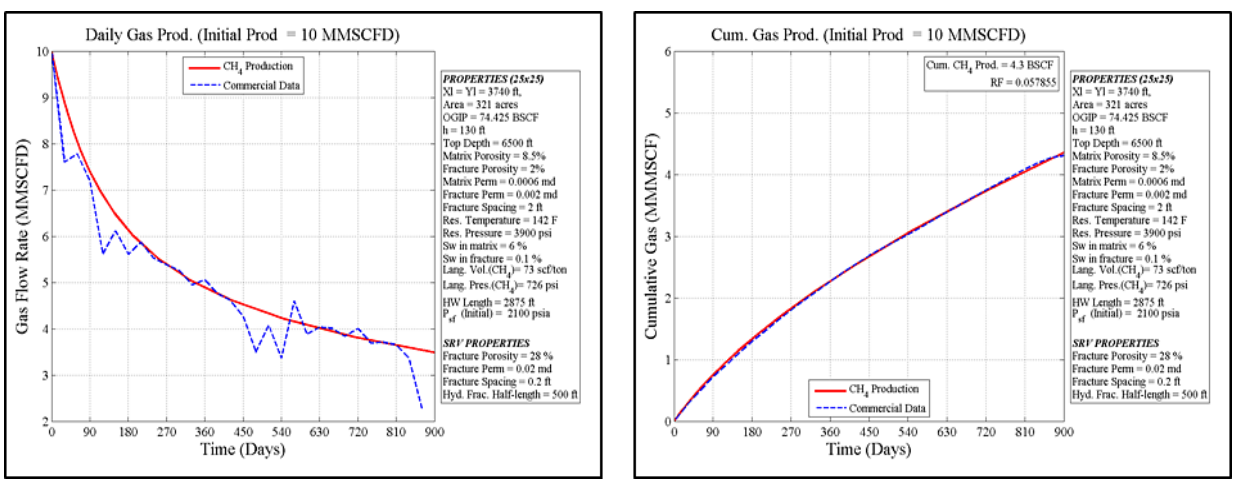

Figure 44: Single-lateral pad, Simulation 4 production performance.

7.2 CO_2 BREAKTHROUGH TIME

An investigation was completed on CO_2 breakthrough time. The same reservoir parameters were used, which are taken from the single lateral problem data in Appendix B. A total of 11 different well spacing values were tested. Figure 45 provides a top view of Models 1 and 11. During the first 30 years, all of the wells were set as production wells. After 30 years, side wells were switched to CO_2 injectors. The center wells keep producing until the BHP reaches 5,000 psi.

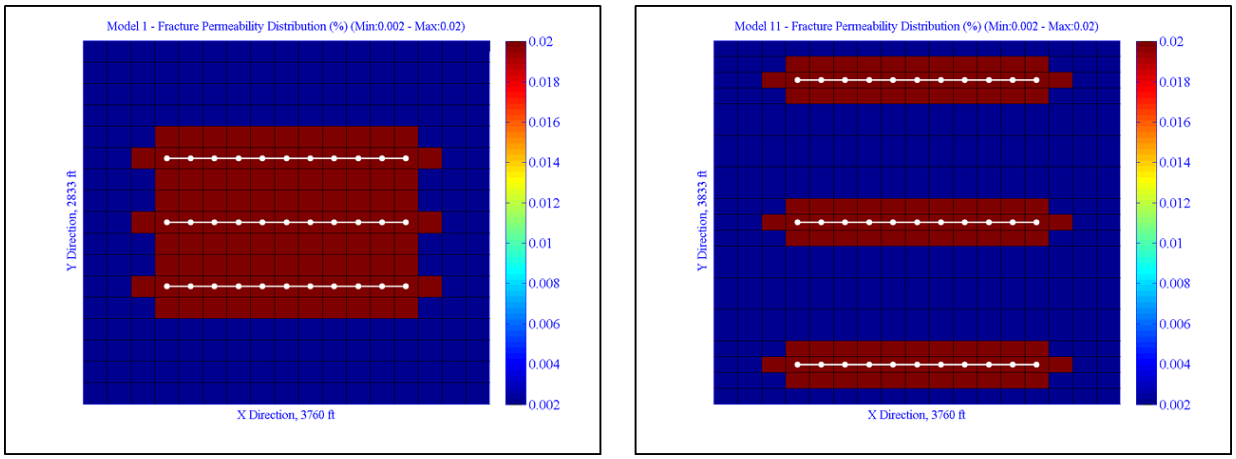

Figure 45: Top view of Model 1 and Model 11.

CO_2 production was observed after about 12 months at the center producer if there was well-established fracture connectivity between wells in the given system, as shown on the left side of Figure 45 (the SRV zones of the injectors and producers are in direct communication). If the unstimulated reservoir volume between the SRVs increases the CO_2 breakthrough times become larger. In some cases, CO_2 breakthrough cannot be seen because the bottomhole pressure constraint ends the simulation (BHP = 5,000 psi).

Figure 46 presents the production performance of 11 different models. The chart on the left is the first 30 years of CH_4 production. After 30 years, side wells are altered to CO_2 injectors. The chart on the right shows the CO_2 breakthrough times for different well spacing values.

CO_2 is observed after about 12 months at the center producer in Model 1 (Model 1 has fracture connectivity between wells). Model 2 has 100 ft of unstimulated zone between SRVs, and starts showing production of CO_2 after about 20 months. In Model 3, there is no fracture connectivity and the distance between SRV regions is 200 ft. CO_2 production is observed after about 24 months.

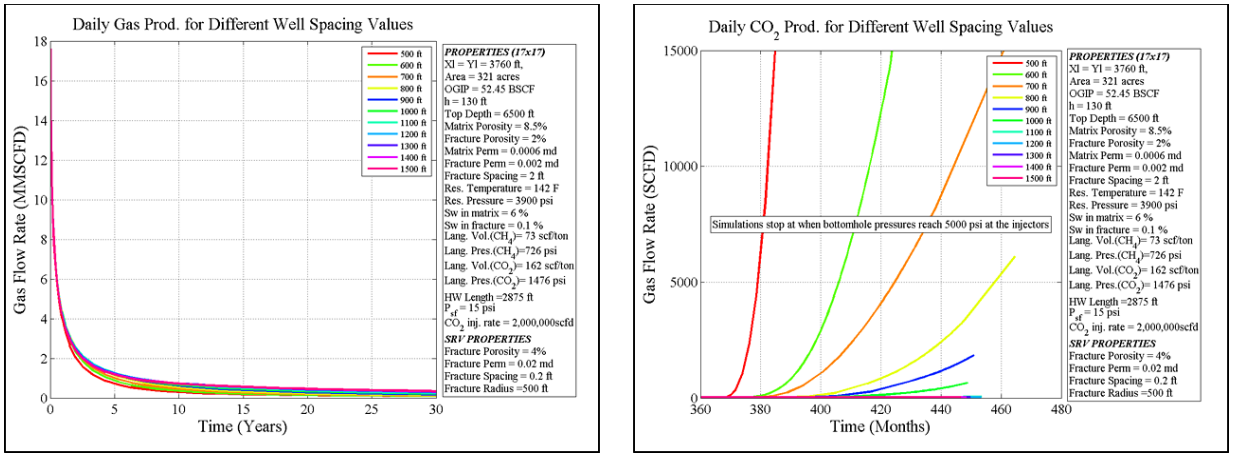

Figure 46: Production performance of Models 1 through 11.

A very small amount of CO_2 is observed at the center producers in Models 4, 5, and 6 due to CO_2 injection at side wells about the 40th, 48th and 55th months, respectively. The simulations stopped because of the BHP constraint at the injectors, which was 5,000 psi.

If the unstimulated reservoir volume between the SRVs gets larger than 500 ft in this set of reservoir models, the CO_2 breakthrough cannot be seen because the BHP constraint ends the simulations (BHP = 5,000 psi). Therefore, from Models 7 through 11, there is no CO_2 production observed after about 8 to 9 years of injection at the center wells.

8. REFERENCES

Bust, V. K.; Majid, A. A.; Oletu, J. U.; Worthington, P. F. In *The Petrophysics of Shale Gas Reservoirs: Technical Challenges and Pragmatic Solutions*, International Petroleum Technology Conference, Bangkok, Thailand, Feb 7–9, **2011**; SPE, Gaffney, Cline & Associates: Bangkok, Thailand, 2011.

Ghaith, A.; Chen, W.; Ortoleva, P. Oscillatory methane release from shale source rock. *Earth-Science Reviews* **1990,** *29*, 241–248.

Hildenbrand, A.; Krooss, B. M. CO_2 migration processes in argillaceous rocks: pressure-driven volume flow and diffusion. In *Journal of Geochemical Exploration*, Fourth International Conference on Fluid Evolution, Migration and Interaction in Sedimentary Basins and Orogenic Belts, **2003**; pp 169–172.

NETL. *Impact of the Marcellus Shale Gas Play on Current and Future CCS Activities*. U.S. Department of Energy, National Energy Technology Laboratory, **2010**.

Siripatrachai, N.; Ertekin, K. Alternate Representations in Numerical Modeling of Multistage Hydraulically Fractured Horizontal Wells in Shale Gas Reservoirs. In *SPE Western Regional Meeting*, Society of Petroleum Engineers: Bakersfield, CA, **2012**.

Vicente, R.; Sarica, C.; Ertekin, T. A Numerical Model Coupling Reservoir and Horizontal Well–Flow Dynamics: Transient Behavior of Single-Phase Liquid and Gas Flow. *Soc. Pet. Eng. J.* **2002,** *7*, 70–77.

Zagorski, W. A.; Bowman, D. C.; Emery, M.; Wrightstone, G. R. An Overview of Some Key Factors Controlling Well Productivity in Core Areas of the Appalachian Basin Marcellus Shale Play; Search and Discovery #110147; **2011**. http://www.searchanddiscovery.com/documents/2011/110147zagorski/ndx_zagorski.pdf

APPENDIX A

ICMI Design Basis Document Tables 3-2 and 3-3

Tables 3-2 and 3-3 are found in the ICMI Design Basis Document. Table 3-2 summarizes modeling parameters for the Northeast Pennsylvania (NE PA) core study area. Table 3-3 summarizes modeling parameters for the Southwest Pennsylvania (SW PA) core study area.

Table 3-2 Modeling Parameters for NE PA Core Study Area Case

Parameter	Range	Source	Comments	Level of Certainty	CO_2 Storage Sensitivity
Reservoir Parameters					
Depth to Marcellus	2,990 – 8,410	IBM GIS	Publicly available GIS data, 5,700 ft average	Medium-High	N/A
Gross thickness (ft)	100 – 500	IBM GIS	Geospatial analysis of publicly available data, 300 ft average	Medium-High	High
Net to gross (NTG) ratio	0.88 – 0.92	WVU (Mohaghegh)	Commercial data, value probably too high	Low-Medium	High
Net thickness (ft)	264 – 276	WVU (Mohaghegh)	Commercial data, calculated average is 270 ft – probably too high	Low-Medium	High
Depth to lateral (ft) – assume midpoint	5,970	WVU (Mohaghegh), IBM GIS	Commercial data, depth to Marcellus plus depth to midpoint	Low-Medium	N/A
Initial pressure gradient, P_i (psi/ft)	0.50 – 0.82	Zagorski et al.	Derived from published data, average = 0.66	Medium	N/A
Initial pressure, P_i (psi)	3,940	Zagorski et al.	Published data used with IBM GIS (average values)	Medium-High	N/A
Initial water saturation, Sw (%)	6 – 13	WVU (Mohaghegh)	Commercial data from SW core	Medium	N/A
Water saturation in matrix, $S_{w\text{-}m}$ (%)	0	WVU (Mohaghegh)	Assume water immobile	Medium	N/A
Water saturation in fracture, $S_{w\text{-}f}$ (%)	0	WVU (Mohaghegh)	Assume water immobile	Medium	N/A
Water relative permeability table (S_w,k_{rw})	See Figure 19	WVU (Mohaghegh)		Low-Medium	N/A
Gas relative permeability table (S_g,k_{rg})	See Figure 19	WVU (Mohaghegh)		Low-Medium	N/A

Parameter	Range	Source	Comments	Level of Certainty	CO_2 Storage Sensitivity
Capillary pressure table (S_w,P_{cow})	See Figure 19	WVU (Mohaghegh)		Low-Medium	N/A
Reservoir temperature, T_i (°F)	142	WVU (Mohaghegh)	Commercial data from SW core	Medium	N/A
CO_2 injection pressure, P_{CO2} (psi) @ 10 % P_i	394	Zagorski et al.	Calculated from P_i at 10 percent	Medium	N/A
Total organic carbon (TOC), weight %	2.6 – 2.8	WVU (Mohaghegh)	Commercial data from SW core	Medium	N/A
Langmuir pressure for CH_4 (psia)	726	WVU (Mohaghegh)	Commercial data from SW core	Medium	N/A
Langmuir volume for CH_4 (scf/ton)	73	WVU (Mohaghegh)	Commercial data from SW core	Medium	N/A
Langmuir pressure for CO_2 (psia)	400	WVU (Mohaghegh)	NETL, 2010	Medium	N/A
Langmuir volume for CO_2 (scf/ton)	14 – 136	WVU (Mohaghegh)	NETL, 2010	Medium	N/A
Matrix porosity, Φ_m (%)	6 – 11	WVU (Mohaghegh)	Commercial data from SW core	Medium	N/A
Matrix permeability, k_m (md)	0.0003 – 0.0009	WVU (Mohaghegh)	Commercial data from SW core	Medium	N/A
Fracture height (ft)	100	WVU (Mohaghegh)	From tables in model	Medium	N/A
Fracture spacing (ft)	0.9 – 2.5	WVU (Mohaghegh)	From tables in model	Medium	N/A
Stimulated reservoir volume (SRV) porosity (%)	0.02 – 2	PSU (Ertekin)	PSU Expert Systems, (Siripatrachai and Ertekin, 2012)	Medium	High
SRV fracture spacing (ft)	0.01 – 0.1	PSU (Ertekin)	PSU Expert Systems, (Siripatrachai and Ertekin, 2012)	Medium	High
Fracture diffusivity on X direction (ft^2/day)	9.3×10^{-4} – 9.3×10^{-6}	PSU (Ertekin)	(Ghaith et al., 1990; Hildenbrand and Krooss, 2003)	Medium	Medium
Fracture diffusivity on Y direction (ft^2/day)	9.3×10^{-4} – 9.3×10^{-6}	PSU (Ertekin)	(Ghaith et al., 1990; Hildenbrand and Krooss, 2003)	Medium	Medium
Fracture diffusivity on Z direction (ft^2/day)	9.3×10^{-4} – 9.3×10^{-6}	PSU (Ertekin)	(Ghaith et al., 1990; Hildenbrand and Krooss, 2003)	Medium	Medium

Parameter	Range	Source	Comments	Level of Certainty	CO_2 Storage Sensitivity
Fracture toughness (psi-in$^{0.5}$)	850–1,200	WVU (Siriwardane), WVU (Mohaghegh	Model assumptions	Medium	N/A
Leakoff Coefficient (ft/min$^{0.5}$)	0.00056 – 0.0015	WVU (Siriwardane), WVU (Mohaghegh	Model assumptions	Medium	N/A
Fracture porosity, Φ_f (%)	0.6 – 1.5	WVU (Mohaghegh)	Commercial data from SW core	Medium	N/A
Fracture permeability, k_f (md)	0.0007 – 0.003	WVU (Mohaghegh)	Commercial data from SW core	Medium	N/A
Swelling/Shrinkage Constant (Palmer & Mansoori model), (tons/scf)	NA	WVU (Siriwardane)	Data needed	N/A	N/A
Sorption Isotherms for Shale-CO_2 interaction	NA	WVU (Siriwardane)	Data needed	N/A	N/A
Sorption time constant (days)	28	WVU (Mohaghegh)	Secondary value from model, history matching	Medium	N/A
Salinity (ppm)	12,000 – 222,000	PSU (Ertekin)	(Bust et al., 2011)	High	Low
Relative Permeability, k_{rel} (md)	NA	WVU (Siriwardane)	Data needed	N/A	N/A
GIP (Bcf/mile)	40 – 180	Zagorski et al.	Commercial data	High	N/A
EUR (Bcf/lateral)	1 – 21	Zagorski et al.	Commercial data	High	N/A
IP (MMcfe/d)	2 – 20	Zagorski et al.	Commercial data	High	N/A
Completion Parameters					
Completed lateral perforated (ft)	2,604 – 3,002	WVU (Mohaghegh)	Commercial data from SW core	Medium	N/A
Completed lateral stimulated (ft)	2,704 – 3,102	WVU (Mohaghegh)	Commercial data from SW core	Medium	N/A
Fracture wing length, (ft)	450 – 600	PSU (Ertekin), WVU (Mohaghegh)	Assumption, calculated using MFrac	Medium	N/A
Number of stages	8 – 10	WVU (Mohaghegh)	Commercial data from SW core	Medium	N/A
Number of clusters/well lateral	24 – 30	WVU (Mohaghegh)	Commercial data from SW core	Medium	N/A
Spacing between stages (ft)	50 – 125	WVU (Mohaghegh)	Commercial data from SW core	Medium	N/A

Parameter	Range	Source	Comments	Level of Certainty	CO_2 Storage Sensitivity
Number of clusters/stage	3	WVU (Mohaghegh)	Commercial data from SW core	Medium	N/A
Shot density (shots/ft)	4	WVU (Mohaghegh)	Commercial data from SW core	Medium	N/A
Amount of pumped proppant (lb/well)	3,794,700 – 5,099,860	WVU (Mohaghegh)	Commercial data from SW core	Medium	N/A
Volume of clean fluid (bbl/well)	100,000 – 125,000	WVU (Mohaghegh)	Commercial data from SW core	Medium	N/A
Stimulation injection rate (bpm)	58.1 – 69.4	WVU (Mohaghegh)	Commercial data from SW core	Medium	N/A
Stimulation injection pressure (psi)	5,883 – 6,145	WVU (Mohaghegh)	Commercial data from SW core	Medium	N/A
Fluid volume (bbl/well)	79,702 – 100,707	WVU (Mohaghegh)	Commercial data from SW core	Medium	N/A
Slurry volume (bbl/well)	113,567 – 144,772	WVU (Mohaghegh)	Commercial data from SW core	Medium	N/A
Fluid density (lb/ft^3)	63.02	WVU (Siriwardane)	Commercial data from SW core	Medium	N/A
Rock Geomechanical Parameters					
Depth to top other layers (ft)	NA	WVU (Siriwardane)	Data needed	N/A	N/A
Thickness of other layers (ft)	NA	WVU (Siriwardane)	Data needed	N/A	N/A
Young's Modulus of Marcellus, E (or shear/bulk modulus) (psi)	2.9×10^6 – 3.6×10^6	WVU (Mohaghegh)	Commercial data, geomechanical logs for SW core	Medium	N/A
Young's modulus of other layers, E (or shear/bulk modulus) (psi)	1,050,000	WVU (Siriwardane)	Data needed	N/A	N/A
Compressibility of each rock type (1/psi)	NA	WVU (Siriwardane)	Data needed	N/A	N/A
Cohesion of each rock type (psi)	NA	WVU (Siriwardane)	Data needed	N/A	N/A
Angle of friction for each rock (degrees)	NA	WVU (Siriwardane)	Data needed	N/A	N/A
Dilation angle for each rock (degrees)	NA	WVU (Siriwardane)	Data needed	N/A	N/A
Tensile strength of each rock (psi)	NA	WVU (Siriwardane)	Data needed	N/A	N/A
Density of Marcellus (lb/ft^3)	159	WVU (Mohaghegh)	Commercial data,	Medium	N/A

Parameter	Range	Source	Comments	Level of Certainty	CO_2 Storage Sensitivity
			geomechanical logs for SW core		
Density of other rocks (lb/ft^3)	NA	WVU (Siriwardane), PSU (Ertekin)	Data needed	N/A	N/A
Poisson's ratio of Marcellus	0.15 – 0.18	WVU (Mohaghegh)	Commercial data, geomechanical logs for SW core	Medium	N/A
Poisson's ratio other rocks	0.25	WVU (Siriwardane)	Data needed	N/A	N/A
Porosity of each rock, $\Phi_{m\,(\%)}$	NA	WVU (Siriwardane)	Data needed	N/A	N/A
Permeability of each rock, k_m (md)	NA	WVU (Siriwardane)	Data needed	N/A	N/A

Table 3-3 Modeling Parameters for SW PA Core Study Area Case

Parameter	Range	Source	Comments	Level of Certainty	CO_2 Storage Sensitivity
Reservoir Parameters					
Depth to Marcellus	6,485 – 6,532	WVU (Mohaghegh)	Commercial data from SW core	High	N/A
Gross thickness (ft)	136 – 148	WVU (Mohaghegh)	Commercial data from SW core	High	High
Net to gross (NTG) ratio	0.88 – 0.92	WVU (Mohaghegh)	Commercial data from SW core	High	High
Net thickness (ft)	125 – 133	WVU (Mohaghegh)	Commercial data from SW core	High	High
Depth to lateral (ft) – assume midpoint	6,610	WVU (Mohaghegh)	Commercial data from SW core	High	N/A
Initial pressure gradient, P_i (psi/ft)	0.59	WVU (Mohaghegh)	Commercial data from SW core	High	N/A
Initial pressure, P_i (psi)	3,890	WVU (Mohaghegh)	Commercial data from SW core	High	N/A
Initial water saturation, Sw (%)	6 – 13	WVU (Mohaghegh)	Commercial data from SW core	High	N/A
Water saturation in matrix, $S_{w\text{-}m}$ (%)	0	WVU (Mohaghegh)	Assume water immobile	Medium	N/A
Water saturation in fracture, $S_{w\text{-}f}$ (%)	0	WVU (Mohaghegh)	Assume water immobile	Medium	N/A
Water relative permeability table (S_w,k_{rw})	See Figure 19	WVU (Mohaghegh)		Low-Medium	N/A
Gas relative permeability table (S_g,k_{rg})	See Figure 19	WVU (Mohaghegh)		Low-Medium	N/A
Capillary pressure table (S_w,P_{cow})	See Figure 19	WVU (Mohaghegh)		Low-Medium	N/A
Reservoir temperature, T_i (°F)	142	WVU (Mohaghegh)	Commercial data from SW core	High	N/A
CO_2 injection pressure, P_{CO2} (psi) @ 10 % P_i	389	WVU (Mohaghegh)	Calculated from P_i at 10%	High	N/A
Total organic carbon (TOC), weight %	2.6 – 2.8	WVU (Mohaghegh)	Commercial data from SW core	High	N/A
Langmuir pressure for CH_4 (psia)	726	WVU (Mohaghegh)	Commercial data from SW core	High	N/A
Langmuir volume for CH_4 (scf/ton)	73	WVU (Mohaghegh)	Commercial data from SW core	High	N/A
Langmuir pressure for CO_2 (psia)	400	WVU (Mohaghegh)	(NETL, 2010)	Medium	N/A
Langmuir volume for CO_2 (scf/ton)	14 – 136	WVU (Mohaghegh)	(NETL, 2010)	Medium	N/A
Matrix porosity, Φ_m (%)	6 – 11	WVU (Mohaghegh)	Commercial data from SW core	High	N/A

Parameter	Range	Source	Comments	Level of Certainty	CO_2 Storage Sensitivity
Matrix permeability, k_m (md)	0.0003 – 0.0009	WVU (Mohaghegh)	Commercial data from SW core	High	N/A
Fracture height (ft)	100	WVU (Mohaghegh)	From tables in model	Medium	N/A
Fracture spacing (ft)	0.9 – 2.5	WVU (Mohaghegh)	From tables in model	Medium	N/A
Stimulated reservoir volume (SRV) porosity (%)	0.02 – 2	PSU (Ertekin)	PSU Expert Systems, (Siripatrachai and Ertekin, 2012)	Medium	High
SRV fracture spacing (ft)	0.01 – 0.1	PSU (Ertekin)	PSU Expert Systems, (Siripatrachai and Ertekin, 2012)	Medium	High
Fracture diffusivity on X direction (ft^2/day)	9.3×10^{-4} – 9.3×10^{-6}	PSU (Ertekin)	(Ghaith et al., 1990; Hildenbrand and Krooss, 2003)	Medium	Medium
Fracture diffusivity on Y direction (ft^2/day)	9.3×10^{-4} – 9.3×10^{-6}	PSU (Ertekin)	(Ghaith et al., 1990; Hildenbrand and Krooss, 2003)	Medium	Medium
Fracture diffusivity on Z direction (ft^2/day)	9.3×10^{-4} – 9.3×10^{-6}	PSU (Ertekin)	(Ghaith et al., 1990; Hildenbrand & Krooss, 2003)	Medium	Medium
Fracture toughness (psi-in$^{0.5}$)	850 – 1,200	WVU (Siriwardane), WVU (Mohaghegh	Model assumptions	Medium	N/A
Leakoff coefficient (ft/min$^{0.5}$)	0.00056 – 0.0015	WVU (Siriwardane), WVU (Mohaghegh	Model assumptions	Medium	N/A
Fracture porosity, Φ_f (%)	0.6 – 1.5	WVU (Mohaghegh)	Commercial data from SW core	High	N/A
Fracture permeability, k_f (md)	0.0007 – 0.003	WVU (Mohaghegh)	Commercial data from SW core	High	N/A
Swelling/shrinkage constant (Palmer & Mansoori model), (tons/scf)	NA	WVU (Siriwardane)	Data needed	N/A	N/A
Sorption isotherms for shale-CO_2 interaction	NA	WVU (Siriwardane)	Data needed	N/A	N/A
Sorption time constant (days)	28	WVU (Mohaghegh)	Secondary value from model, history matching	Medium	N/A
Salinity (ppm)	12,000 – 222,000	PSU (Ertekin)	(Bust et al., 2011)	High	Low
Relative permeability, k_{rel} (md)	NA	WVU (Siriwardane)	Data needed	N/A	N/A

Parameter	Range	Source	Comments	Level of Certainty	CO_2 Storage Sensitivity
GIP (Bcf/mile)	40 – 150	Zagorski et al.	Commercial data	High	N/A
EUR (Bcf/lateral)	2 to > 12	Zagorski et al.	Commercial data	High	N/A
IP (MMcfe/d)	1 to > 21	Zagorski et al.	Commercial data	High	N/A
Completion Parameters					
Completed lateral perforated (ft)	2,604 – 3,002	WVU (Mohaghegh)	Commercial data from SW core	High	N/A
Completed lateral stimulated (ft)	2,704 -,3,102	WVU (Mohaghegh)	Commercial data from SW core	High	N/A
Fracture wing length, (ft)	450 – 600	PSU (Ertekin), WVU (Mohaghegh)	Assumption, calculated using MFrac	Medium	N/A
Number of stages	8 – 10	WVU (Mohaghegh)	Commercial data from SW core	High	N/A
Number of clusters/well lateral	24 – 30	WVU (Mohaghegh)	Commercial data from SW core	High	N/A
Spacing between stages (ft)	50 – 125	WVU (Mohaghegh)	Commercial data from SW core	High	N/A
Number of clusters/stage	3	WVU (Mohaghegh)	Commercial data from SW core	High	N/A
Shot density (shots/ft)	4	WVU (Mohaghegh)	Commercial data from SW core	High	N/A
Amount of pumped proppant (lb/well)	3,794,700 – 5,099,860	WVU (Mohaghegh)	Commercial data from SW core	High	N/A
Volume of clean fluid (bbl/well)	100,000 – 125,000	WVU (Mohaghegh)	Commercial data from SW core	High	N/A
Stimulation injection rate (bpm)	58.1 – 69.4	WVU (Mohaghegh)	Commercial data from SW core	High	N/A
Stimulation injection pressure (psi)	5,883 – 6,145	WVU (Mohaghegh)	Commercial data from SW core	High	N/A
Fluid volume (bbl/well)	79,702 – 100,707	WVU (Mohaghegh)	Commercial data from SW core	High	N/A
Slurry volume (bbl/well)	113,567 – 144,772	WVU (Mohaghegh)	Commercial data from SW core	High	N/A
Fluid density (lb/ft^3)	63.02	WVU (Siriwardane)	Commercial data from SW core	High	N/A

Parameter	Range	Source	Comments	Level of Certainty	CO_2 Storage Sensitivity
Rock Geomechanical Parameters					
Depth to top other layers (ft)	NA	WVU (Siriwardane)	Data needed	N/A	N/A
Thickness of other layers (ft)	NA	WVU (Siriwardane)	Data needed	N/A	N/A
Young's modulus of Marcellus, E (or shear/bulk modulus) (psi)	2.9×10^6 – 3.6×10^6	WVU (Mohaghegh)	Commercial data, geomechanical logs for SW core	High	N/A
Young's Modulus of other layers, E (or shear/bulk modulus) (psi)	1,050,000	WVU (Siriwardane)	Data needed	N/A	N/A
Compressibility of each rock type (1/psi)	NA	WVU (Siriwardane)	Data needed	N/A	N/A
Cohesion of each rock type (psi)	NA	WVU (Siriwardane)	Data needed	N/A	N/A
Angle of friction for each rock (degrees)	NA	WVU (Siriwardane)	Data needed	N/A	N/A
Dilation angle for each rock (degrees)	NA	WVU (Siriwardane)	Data needed	N/A	N/A
Tensile strength of each rock (psi)	NA	WVU (Siriwardane)	Data needed	N/A	N/A
Density of Marcellus (lb/ft^3)	159	WVU (Mohaghegh)	Commercial data, geomechanical logs for SW core	High	N/A
Density of other rocks (lb/ft^3)	NA	WVU (Siriwardane), PSU (Ertekin)	Data needed	N/A	N/A
Poisson's ratio of Marcellus	0.15 – 0.18	WVU (Mohaghegh)	Commercial data, geomechanical logs for SW core	High	N/A
Poisson's ratio other rocks	0.25	WVU (Siriwardane)	Data needed	N/A	N/A
Porosity of each rock, $\Phi_{m\,(\%)}$	NA	WVU (Siriwardane)	Data needed	N/A	N/A
Permeability of each rock, k_m (md)	NA	WVU (Siriwardane)	Data needed	N/A	N/A

APPENDIX B

Single-Lateral Problem Data

Single-Lateral Problem Parameters and Values

Parameters	Values
Initial production (MMSCFD)	10
Grid system	Model specific
Grid size on X direction (ft)	Model specific
Grid size on Y direction (ft)	Model specific
Reservoir dimension X (ft)	3,740
Reservoir dimension Y (ft)	3,740
Area (acres)	321
NET thickness (ft)	130
Depth to Marcellus (ft)	6,500
Minimum depth to lateral (ft) – assume midpoint	6,600
Matrix porosity (%)	8.5
Fracture porosity (%)	2
Matrix permeability (md)	0.0006
Fracture permeability (md)	0.002
Fracture spacing (ft)	2.0
Reservoir temperature (°F)	142
Reservoir pressure (psi)	3,900
Water saturation in matrix (%)	6
Sw in fracture (%)	0, approximately
Langmuir volume of CH_4 (scf/ton)	73
Langmuir pressure of CH_4 (psi)	726
Langmuir volume of CO_2 (scf/ton)	75
Langmuir pressure of CO_2 (psi)	400
Horizontal wellbore length (ft)	2,875
Sandface pressure (psi)	550, trial-and-error (Eclipse) to match IP
SRV fracture porosity (%)	2.0
SRV fracture permeability (md)	0.0185
Hydro-fracture permeability (md-ft)	3.0
SRV fracture spacing (ft)	0.2
Completed lateral perforated (horizontal wellbore length [ft])	2,875
Hydraulic fracture half-length (ft) (wing length)	500
Number of stages	8
Spacing between stages	350
Number of clusters/well lateral	24
Spacing between clusters	100

Note: Simulation time = 100 years in 5-year steps

Sean Plasynski
Director
Strategic Center for Coal
National Energy Technology Laboratory
U.S. Department of Energy

Traci Rodosta
Sequestration Technology Manager
Strategic Center for Coal
National Energy Technology Laboratory
U.S. Department of Energy

Cynthia Powell
Director
Office of Research and Development
National Energy Technology Laboratory
U.S. Department of Energy

George Richards
Focus Area Lead
Energy Systems Dynamics
National Energy Technology Laboratory
U.S. Department of Energy

Angela Goodman
Technical Project Lead
Carbon Storage Materials
Characterization Division
National Energy Technology Laboratory
U.S. Department of Energy

Kevin Donovan
RES Program Manager
URS Corporation